CALET

Calorimetric
Electron
Telescope

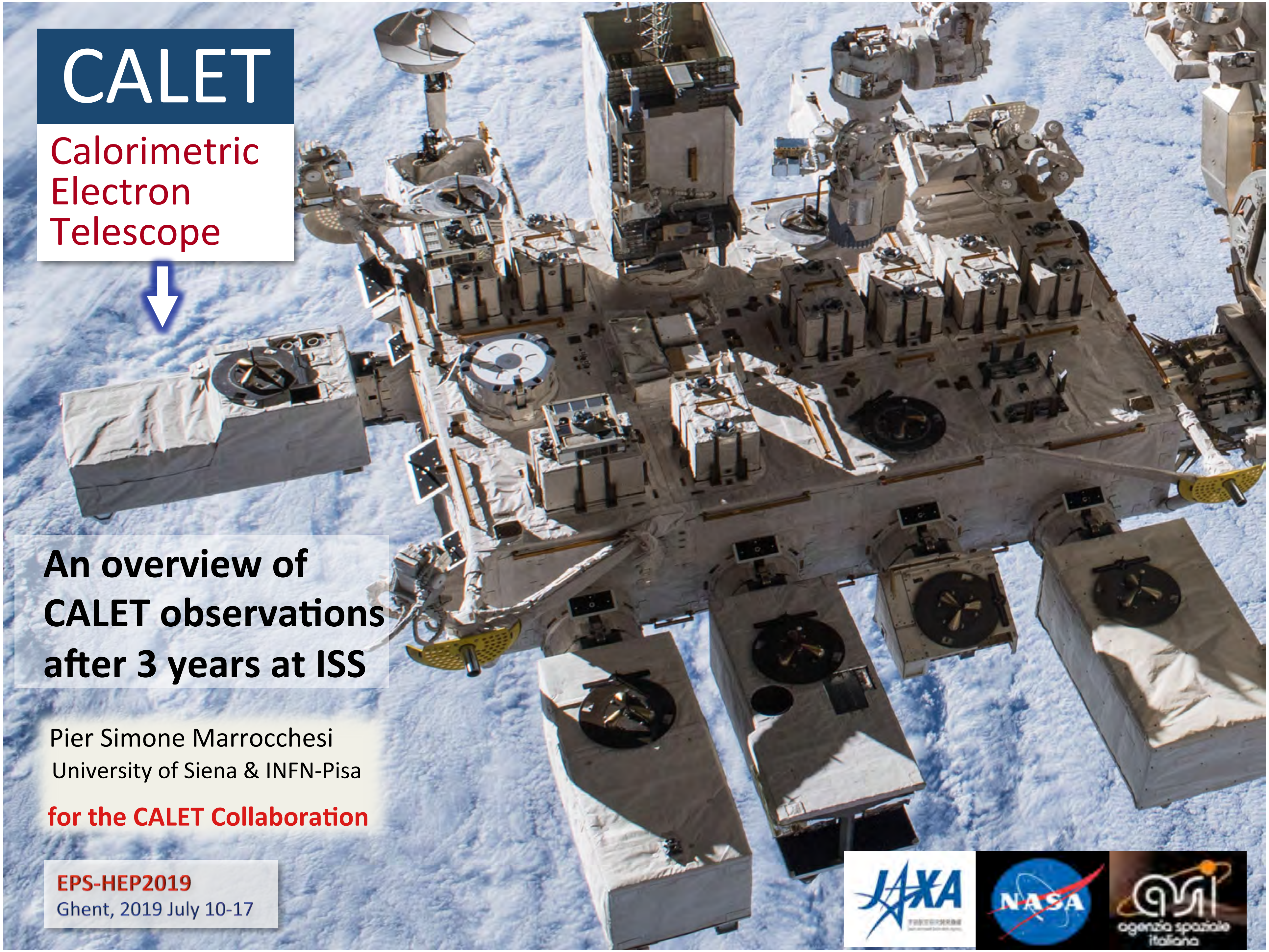

An overview of CALET observations after 3 years at ISS

Pier Simone Marrocchesi
University of Siena & INFN-Pisa

for the CALET Collaboration

EPS-HEP2019
Ghent, 2019 July 10-17

CALET Payload

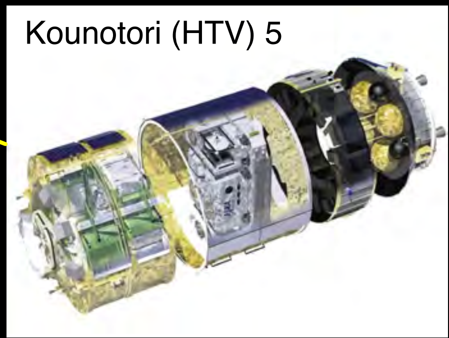

Launched on Aug. 19th, 2015 by the Japanese H2-B rocket

Emplaced on port #9 of JEM-EF (Japanese Experiment Module Exposed Facility) on Aug. 25th

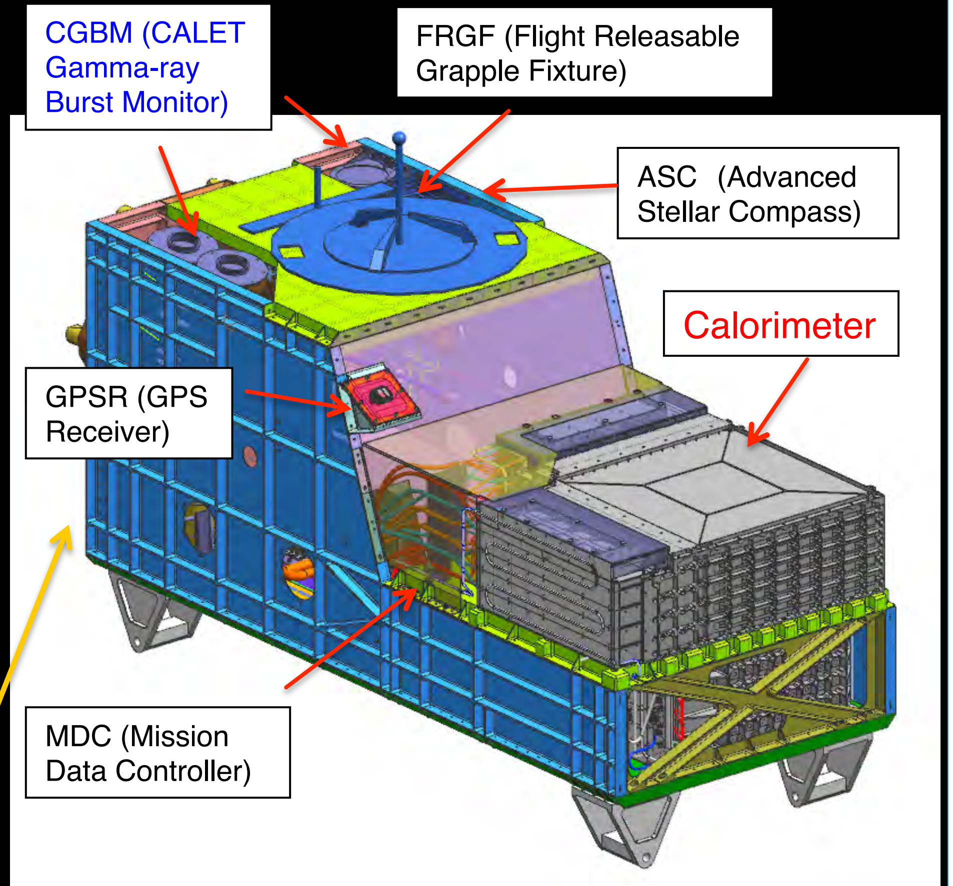

- Mass: 612.8 kg JEM Standard Payload
- Size: 1850mm (L) × 800mm (W) × 1000mm (H)
- Power: 507 W (max)
- Telemetry: Medium 600 kbps (6.5GB/day)

Cosmic Ray Observations aboard the ISS and CALET program

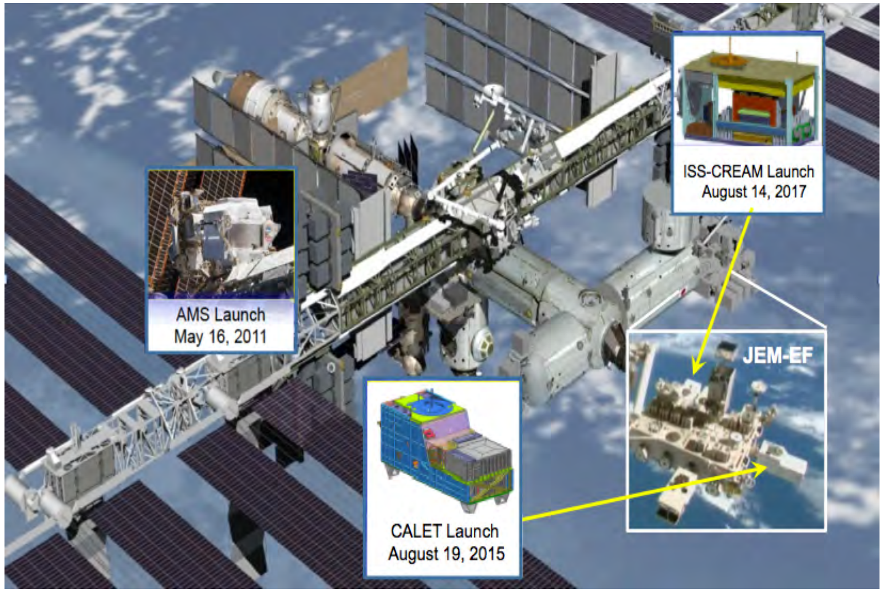

Main CALET science objectives:

- ✧ **Electron observation** in 1 GeV - 20 TeV range.
  Design optimized for electron detection: high energy resolution and large e/p separation power + e.m. shower containment. Detailed study of spectral shape.
  Search for Dark Matter and Nearby Sources
- ✧ **Observation of cosmic-ray nuclei** in the energy region from 10 GeV to 1 PeV.
  Unravelling the CR acceleration and propagation mechanism(s)
- ✧ Detection of **transient phenomena** in space
  Gamma-ray bursts, e.m. GW counterparts, Solar flares, Space Weather

Scientific Objectives	Observation Targets	Energy Range
CR Origin and Acceleration	Electron spectrum Individual spectra of elements from proton to Fe Ultra Heavy Ions ($26 < Z \leq 40$) Gamma-rays (Diffuse + Point sources)	1GeV - 20 TeV 10 GeV - 1000 TeV > 600 MeV/n 1 GeV - 1 TeV
Galactic CR Propagation	B/C and sub-Fe/Fe ratios	Up to some TeV/n
Nearby CR Sources	Electron spectrum	100 GeV - 20 TeV
Dark Matter	Signatures in electron/gamma-ray spectra	100 GeV - 20 TeV
Solar Physics	Electron flux (1GeV-10GeV)	< 10 GeV
Gamma-ray Transients	Gamma-rays and X-rays	7 keV - 20 MeV

CALET instrument in a nutshell

Field of view: ~ 45 degrees (from the zenith) Geometrical Factor: ~ 1,040 $cm^2 sr$ (for electrons)

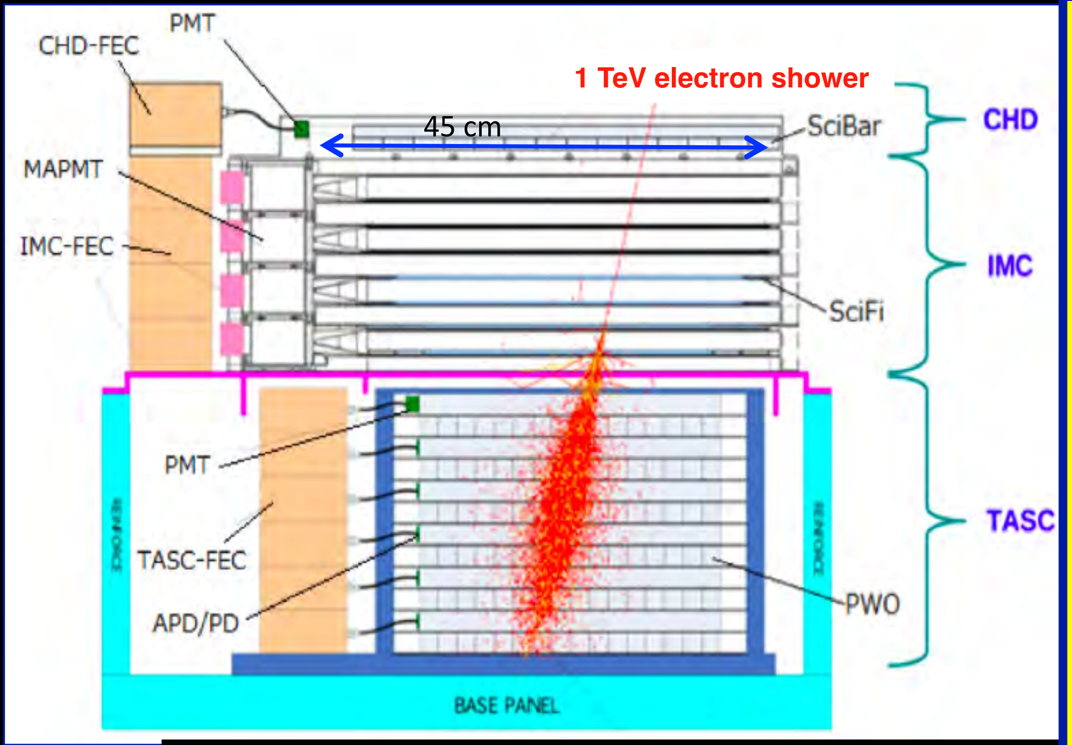

CALET: a unique set of key instruments

- **CHD**: a dedicated charge detector + multiple dE/dx sampling in the IMC allow the **identification of individual nuclear species** (charge resolution ~0.15-0.3 e).
- **IMC**: high granularity (1mm) imaging pre-shower calorimeter to accurately reconstruct **the arrival direction** of incident particles (~0.1°) and the **starting point** of electro-magnetic showers.
  Scifi + Tungsten absorbers: **3 X_0** (=0.2 X_0 x 5 + 1.0 X_0 x 2)
- **TASC**: thick (**27 X_0**) homogeneous PWO calorimeter allowing to extend electron measurements into the TeV energy region with ~2% **energy resolution**.
- **Combined** (**30 X_0, 1.2 λ_I**) they **separate electrons** from the abundant protons (rejection > 10^5).

Simulated Shower Profile

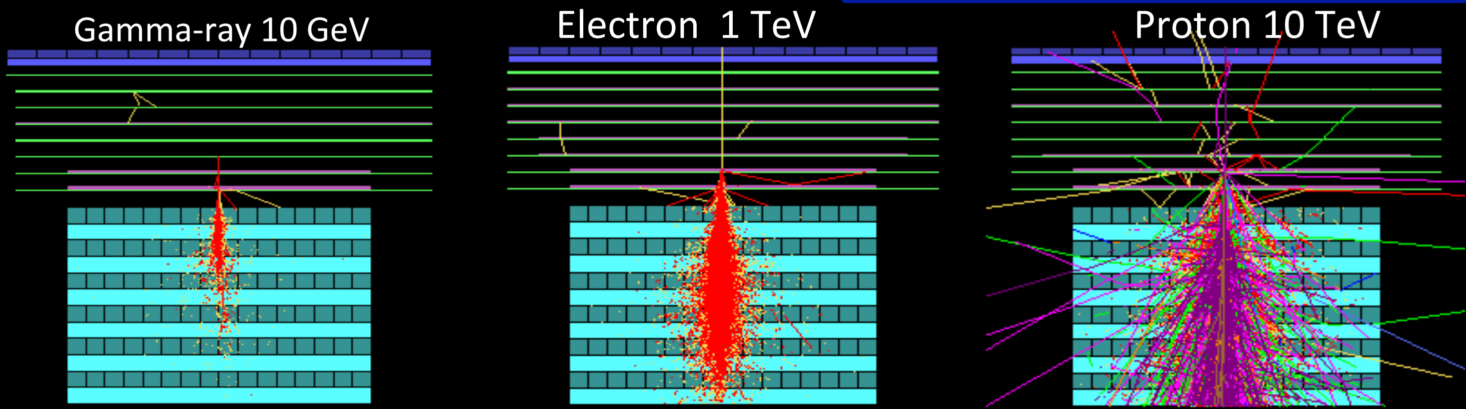

Examples of Observed Events

Multi-prong background event (interaction in CHD)

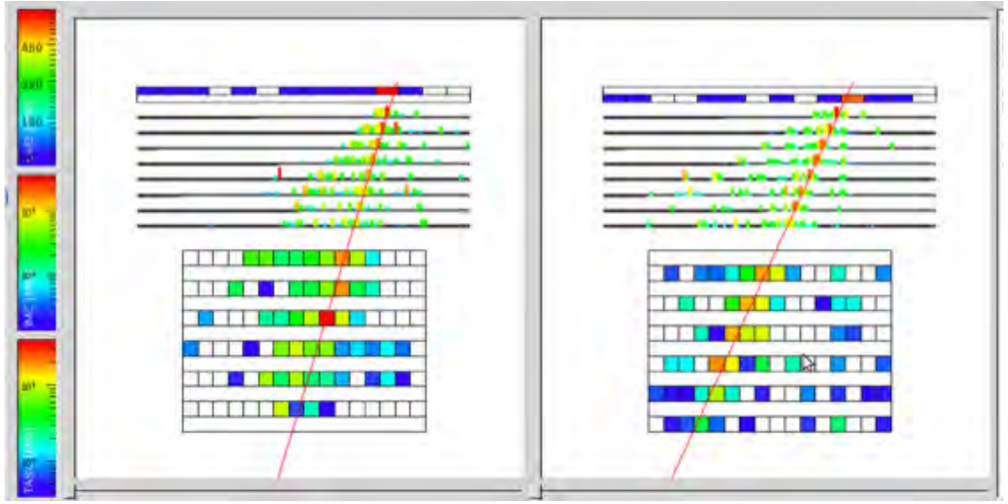

Proton, ΔE=2.89 TeV

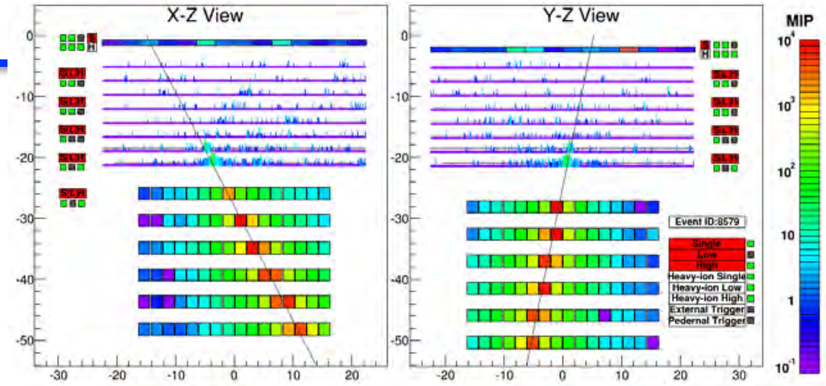

Iron, ΔE=9.3 TeV

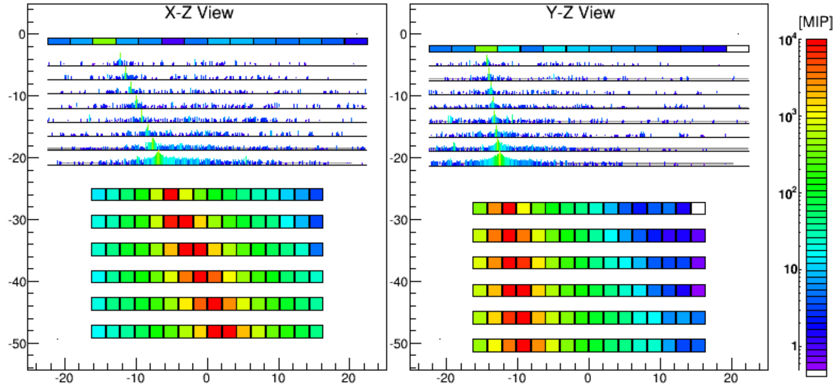

Electron, E=3.05 TeV

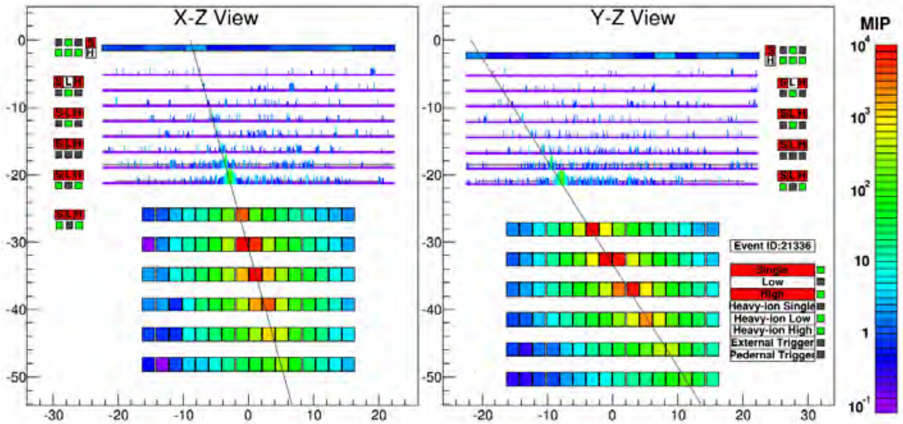

Gamma-ray, E=44.3

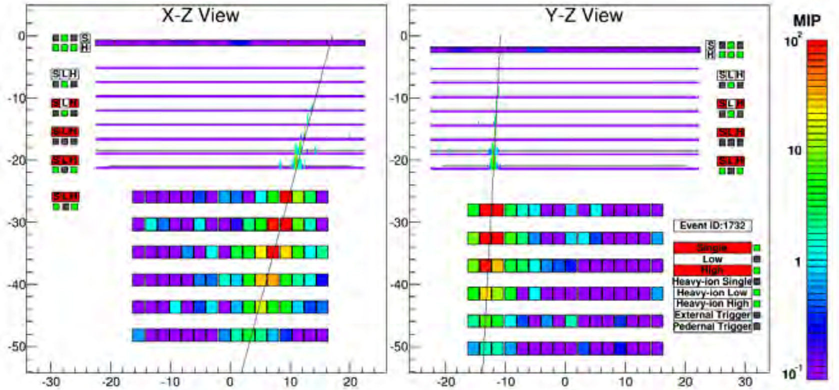

CALET Instrument overview

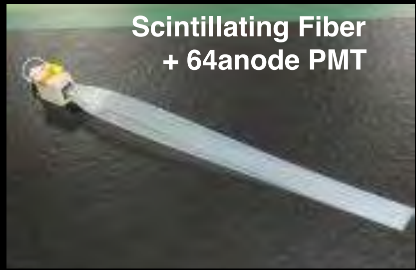

CALORIMETER

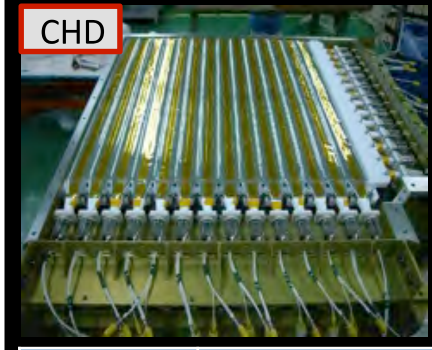

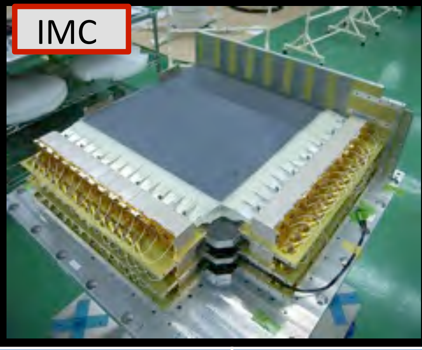

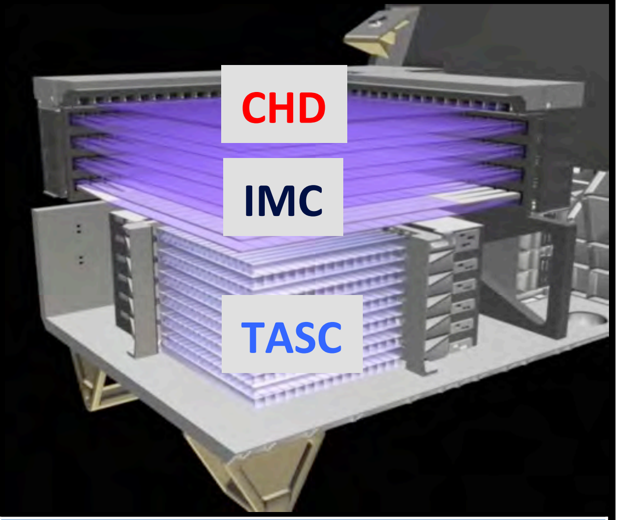

	CHD (Charge Detector)	IMC (Imaging Calorimeter)	TASC (Total Absorption Calorimeter)
Measure	**Charge (Z=1-40)**	**Tracking , Particle ID**	**Energy, e/p Separation**
Geometry (Material)	**Plastic Scintillators**: 28 paddles 14 paddles x 2 layers (X,Y) Paddle Size: 32 x 10 x 450 mm^3	**Scintillating Fibers**: 448 x 16 layers (X,Y) Scifi size: 1 x 1 x 448 mm^3 7 Tungsten layers : 0.2X_0 x 5 + 1X_0 x 2 Total Thickness: **3 X_0**	**PWO logs**: 16 x 12 layers (x,y): 192 logs log size: 19 x 20 x 326 mm^3 Total Thickness: **27 X_0 , ~1.2 λ_I**
Readout	**PMT+CSA**	**64-anode PMT+ ASIC**	**APD/PD+CSA** **PMT+CSA (for Trigger)@top layer**

Energy Measurement in a wide dynamic range 1-10^6 MIPs

"MIP" peak in PWO: Obs. vs. MC

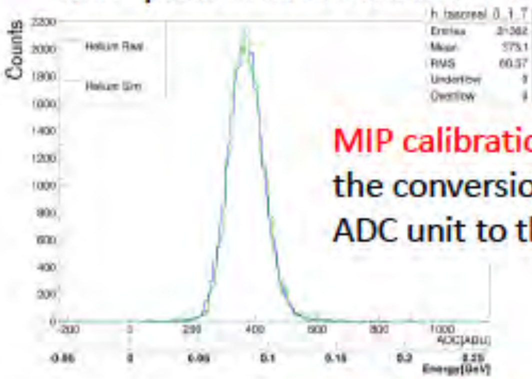

MIP calibration determines the conversion factor from ADC unit to the energy

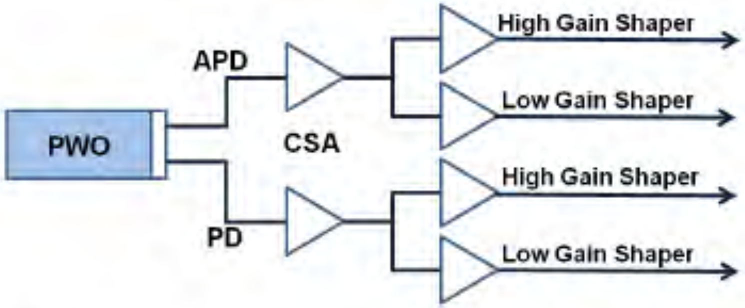

The whole dynamic range was calibrated by UV laser irradiation on ground :

1) The linearity of each gain range is confirmed in the range of 1.4-2.5 %.

2) Each channel covers from 1 MIP to 10^6 MIPs.

APD-H	APD-L	PD-H	PD-L
1.4%	1.5%	2.5%	2.2%

The correlation between adjacent gain ranges is calibrated by using in-flight data in each channel.

APD-H APD-L	APD-L PD-H	PD-H PD-L
0.1%	0.7%	0.1%

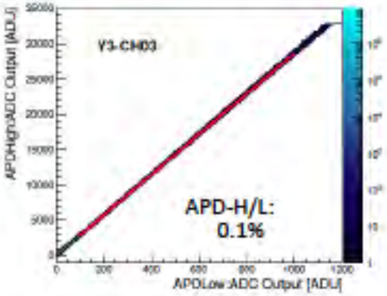

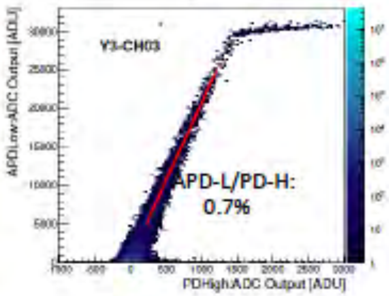

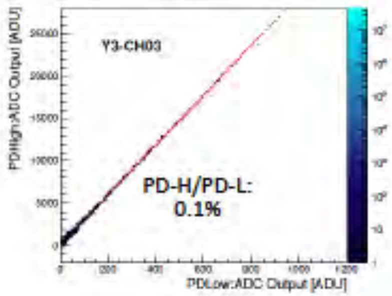

Example of energy distribution in one PWO log

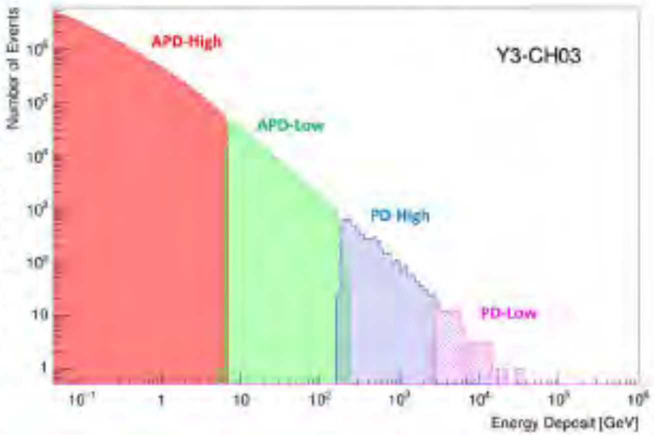

Observations with High Energy Trigger (>10GeV)

Observation with High Energy Trigger for 1327 days : Oct.13, 2015 – May 31, 2019

- The exposure, SΩT, has reached ~116 m^2 sr day for electron observations under continuous and stable operations.
- Total number of triggered events is ~1.8 billion with a live time fraction of ~84 %.

Accumulated observation time (live, dead)

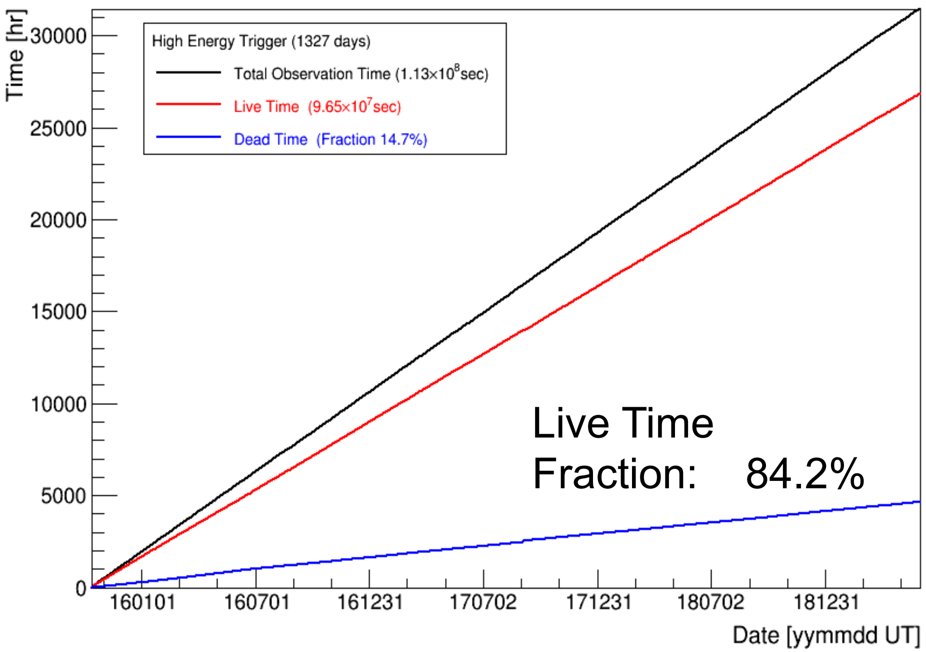

Distribution of deposit energies (ΔE) in TASC

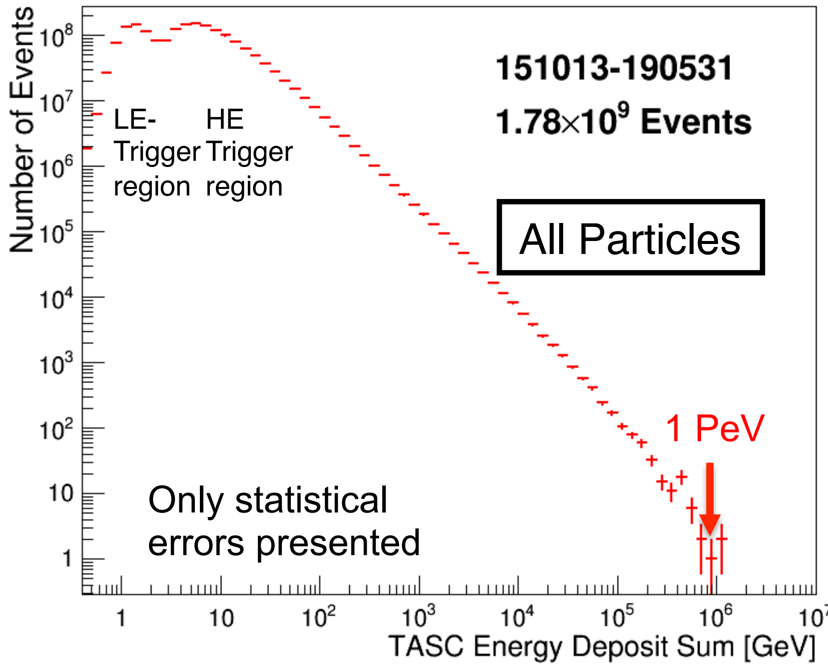

Position and Temperature Calibration + Long-term Stability

Example of position dependence correction

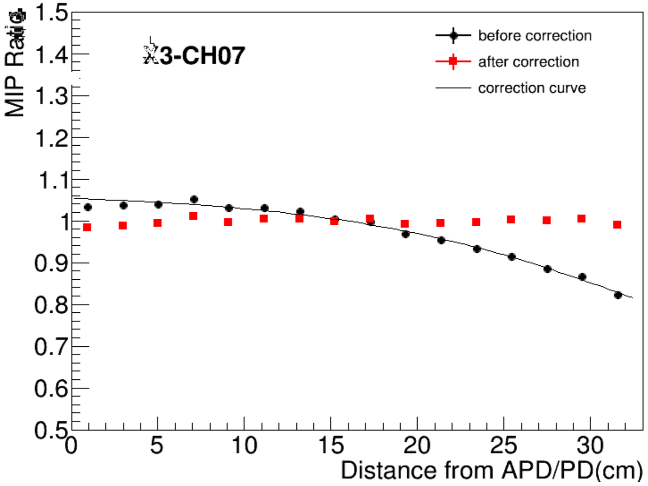

Examples of temperature change correction

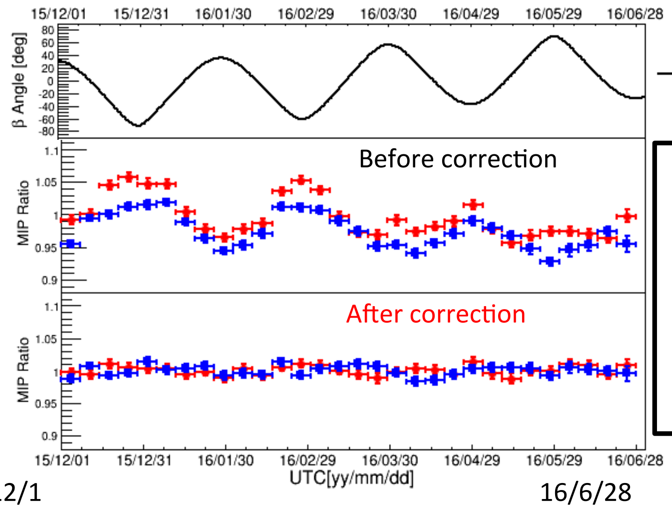

15/12/1 16/6/28

TASC

Active Thermal Control System (ATCS) on ISS provides very stable thermal conditions during long-tem observations: Δt ~ a few degrees

Energy Resolution for Electrons by On-orbit Calibration

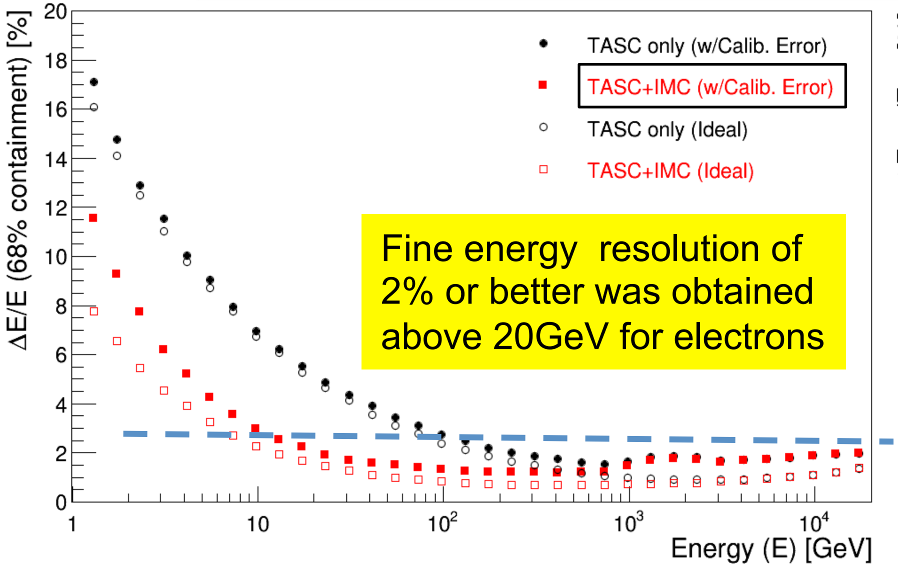

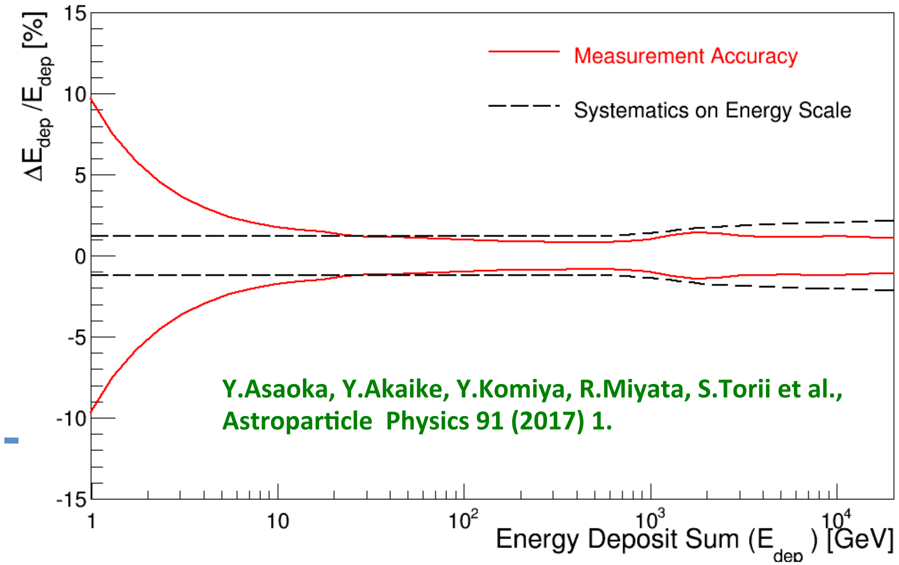

Electron / Proton Discrimination [Y.Asaoka, COSPAR 2108 E1.5-0023-18]

Simple Two Parameter Cut

F_E: Energy fraction of the bottom layer sum to the whole energy deposit sum in TASC

R_E: Lateral spread of energy deposit in TASC-X1

Cut Parameter K is defined as follows:

$K = \log_{10}(F_E) + 0.5\ R_E$ (/cm)

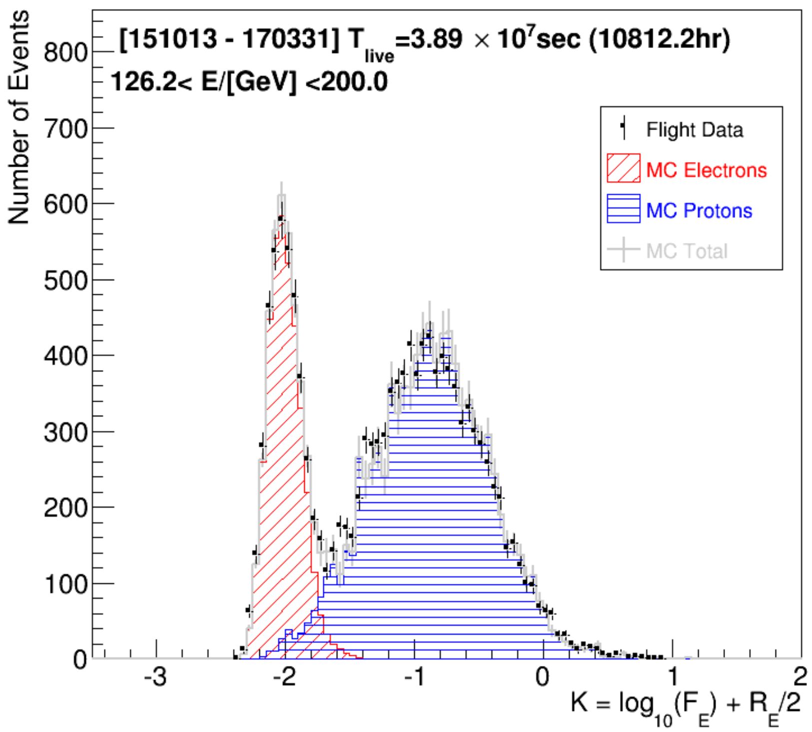

Boosted Decision Trees (BDT)

In addition to the two parameters on the left, TASC and IMC shower profile fits are used as discriminating variables

BDT Response using 9 parameters

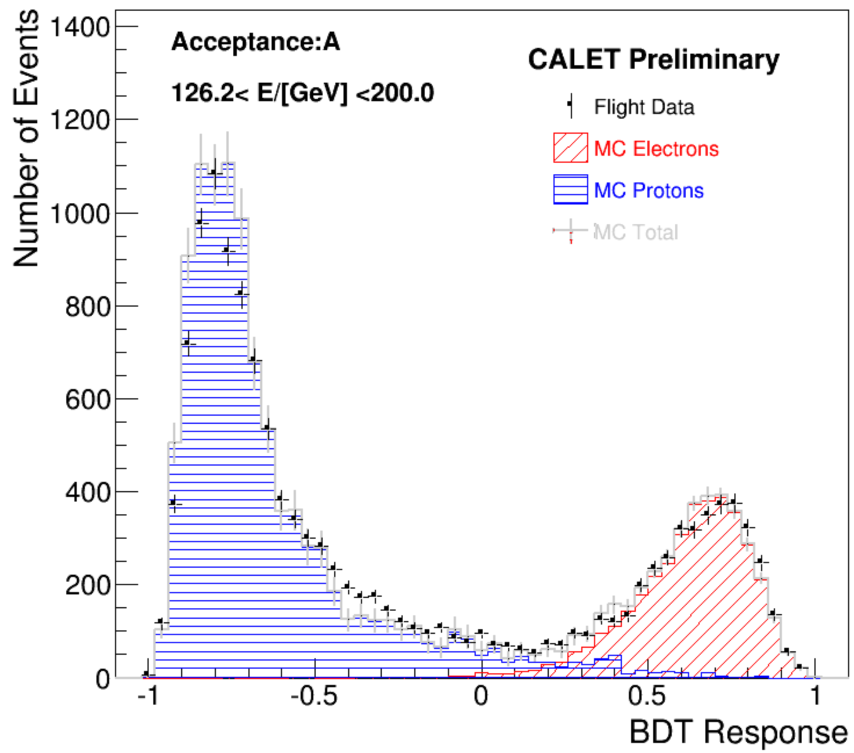

Cutoff Rigidity Measurements and Comparison with Calculation

BEFORE CORRECTION

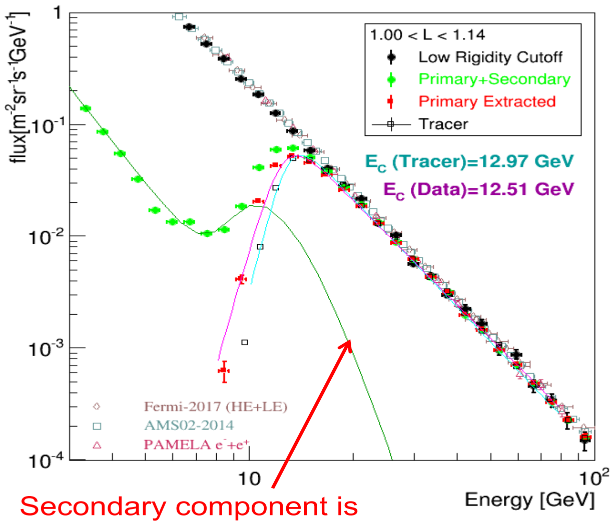

Secondary component is estimated using azimuthal distributions

AFTER CORRECTION

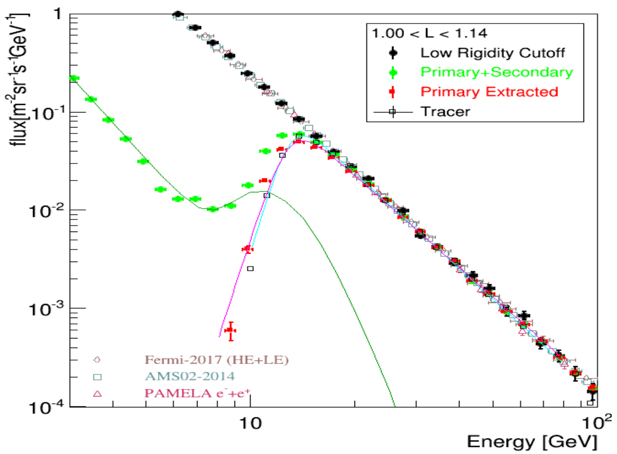

- Performed in three different cutoff rigidity regions.
- Correction factor was found to be **1.035** compared to MIP calibration.

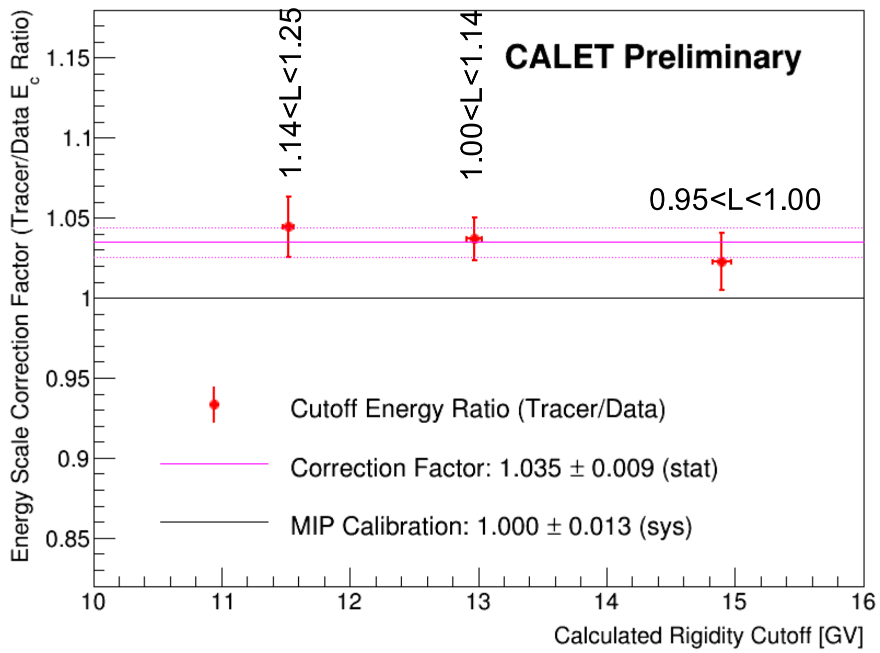

[Y.Asaoka, COSPAR 2018 E1.5-0023-18]

[S.Miyake, COSPAR 2018 E1.5-0027-18]

Systematic Uncertainties (electron spectrum)

Stability of resultant flux analyzed by scanning parameter space

- **Normalization:**
  - Live time
  - Radiation environment
  - Long-term stability
  - Quality cuts
- **Energy dependent:**
  - 2 independent tracking
  - charge ID
  - electron ID (K-Cut vs BDT)
  - MC model (EPICS vs Geant4)
  - BDT stability (vs efficiency & training)

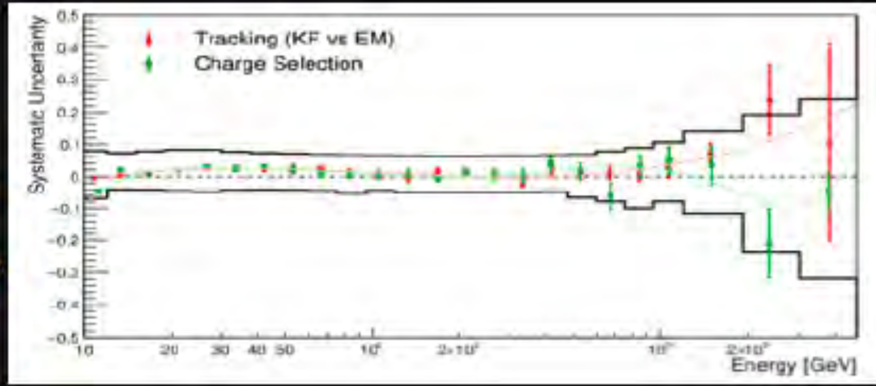

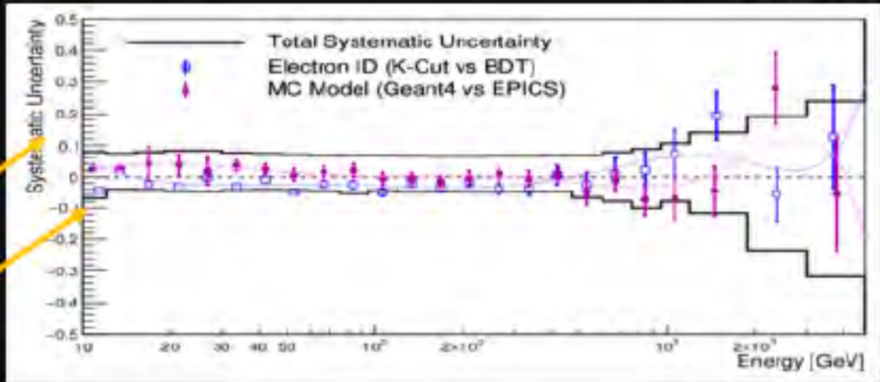

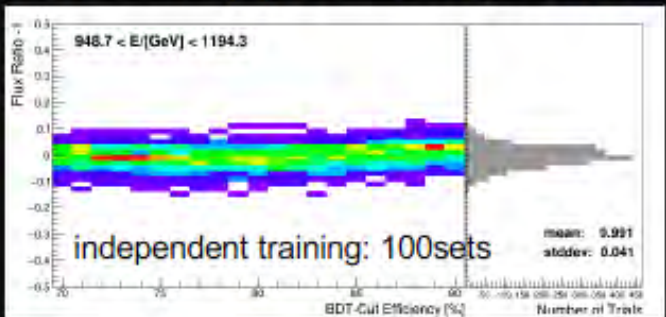

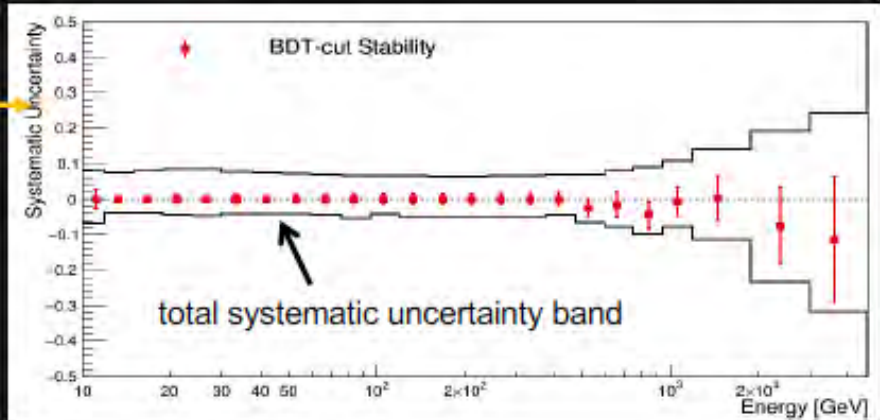

Direct measurements of the electron spectrum

Comparison of CALET with DAMPE and other experiments in space

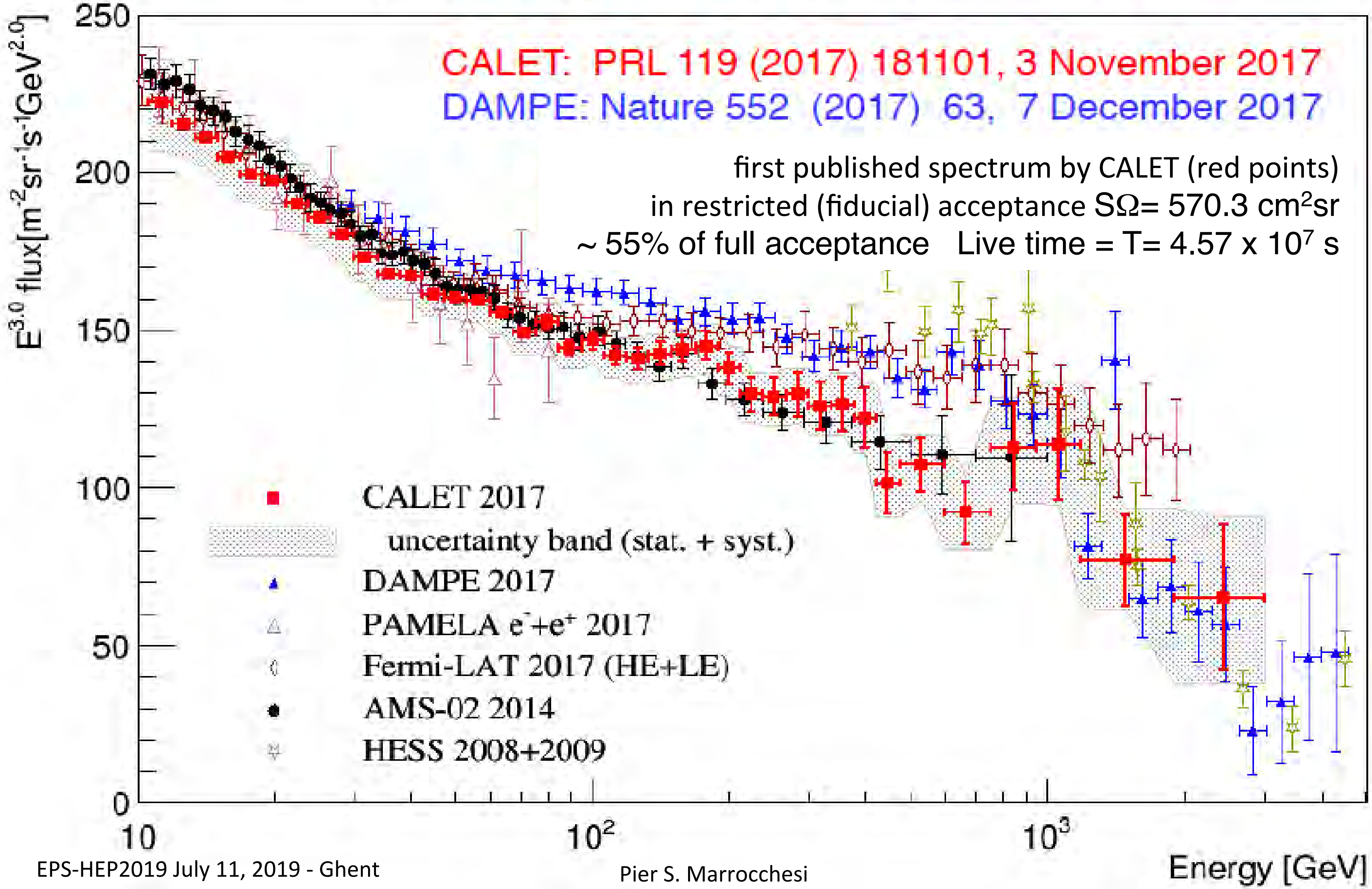

Extended CALET measurement of electron spectrum

Approximately doubled statistics above 500GeV by using full acceptance of CALET

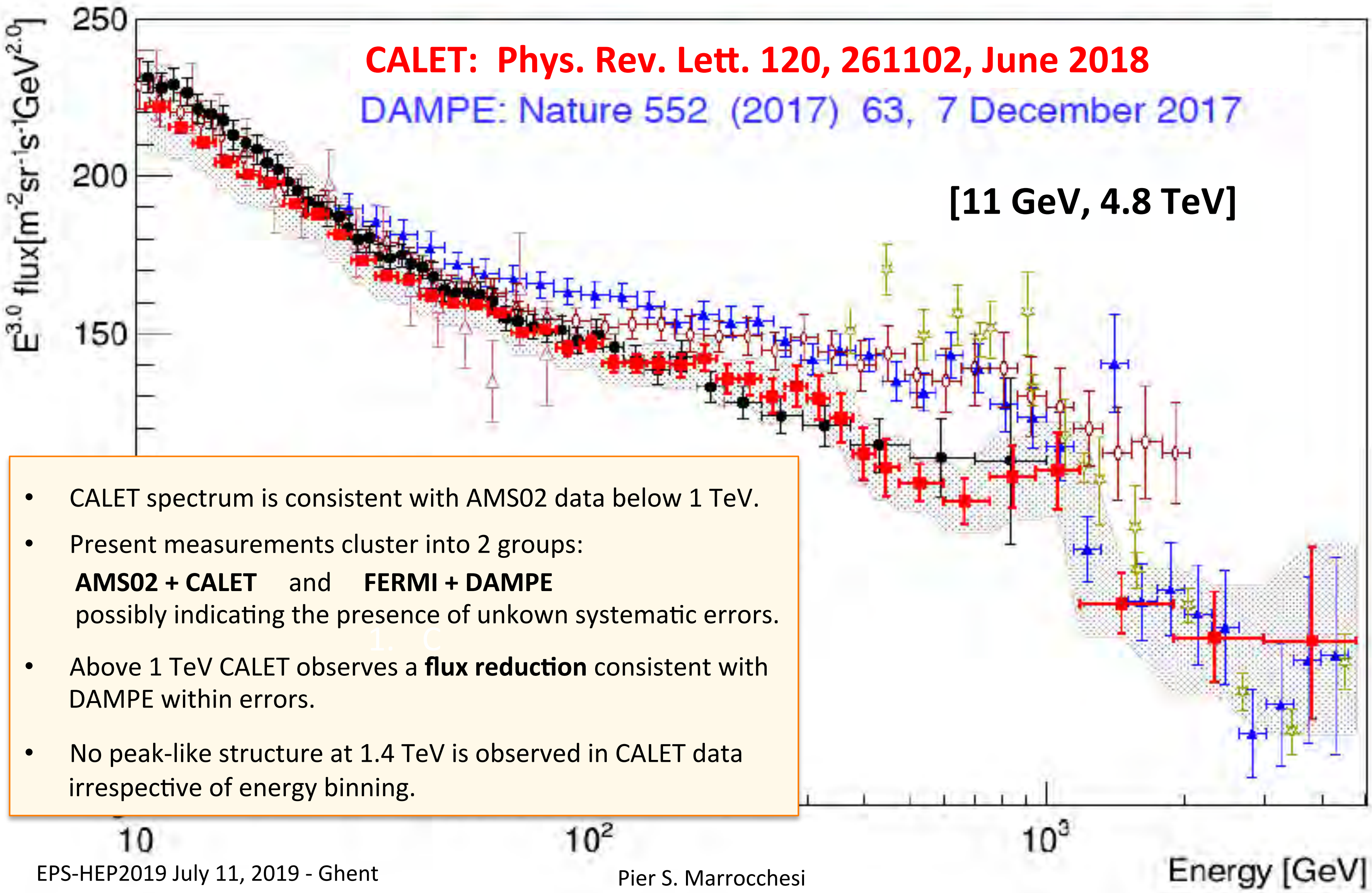

- CALET spectrum is consistent with AMS02 data below 1 TeV.
- Present measurements cluster into 2 groups:
  AMS02 + CALET and **FERMI + DAMPE**
  possibly indicating the presence of unkown systematic errors.
- Above 1 TeV CALET observes a **flux reduction** consistent with DAMPE within errors.
- No peak-like structure at 1.4 TeV is observed in CALET data irrespective of energy binning.

Direct measurement of proton spectrum by CALET

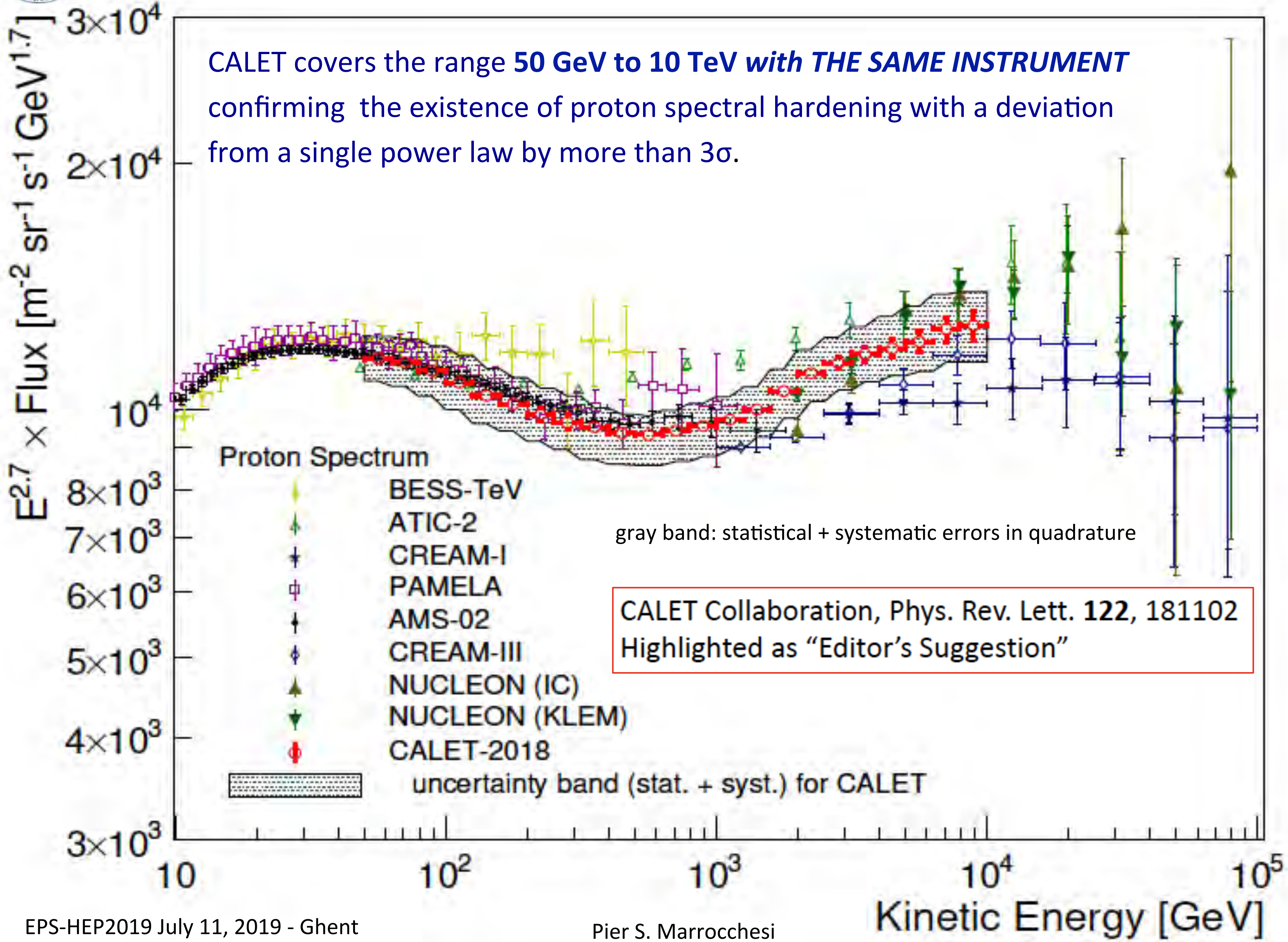

Spectral Behavior of Proton Flux

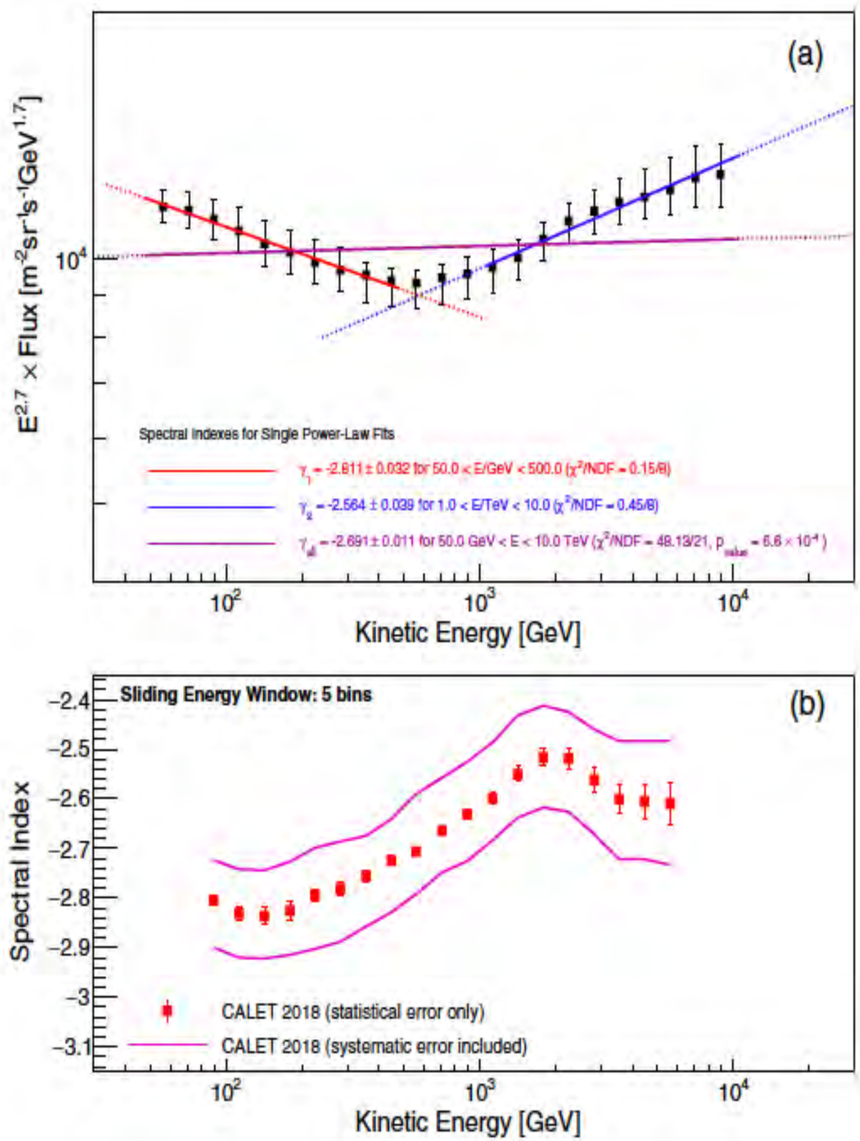

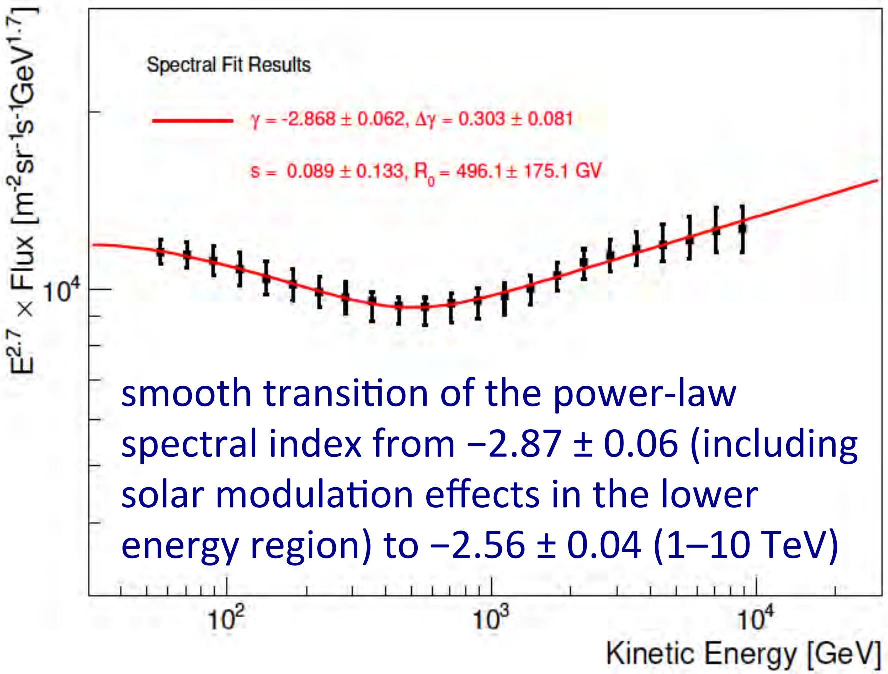

smooth transition of the power-law spectral index from −2.87 ± 0.06 (including solar modulation effects in the lower energy region) to −2.56 ± 0.04 (1–10 TeV)

1. Subranges of 50—500GeV, 1-10TeV can be fitted with single power law function, but not the whole range (significance > 3σ).
2. Progressive hardening up to the TeV region was observed.
3. "smoothly broken power-law fit" gives power law index consistent with AMS-02 in the low energy region, but shows larger index change and higher break energy than AMS-02.

Direct measurements of proton spectrum to date

- ✧ **p and He below 100 GeV:** % level agreement of magnetic spectrometers (**BESS-TeV, PAMELA, AMS02**)
- ✧ good agreement of PAMELA and AMS-02 on p and He spectra **below a few hundred GeV.**
- ✧ The next challenge is the region from **10 TeV to 100 TeV** being explored by balloon-borne (e.g.: **ATIC, CREAM**) and space instruments (**CALET, DAMPE, NUCLEON**).
  To date, published results in this region have large errors.

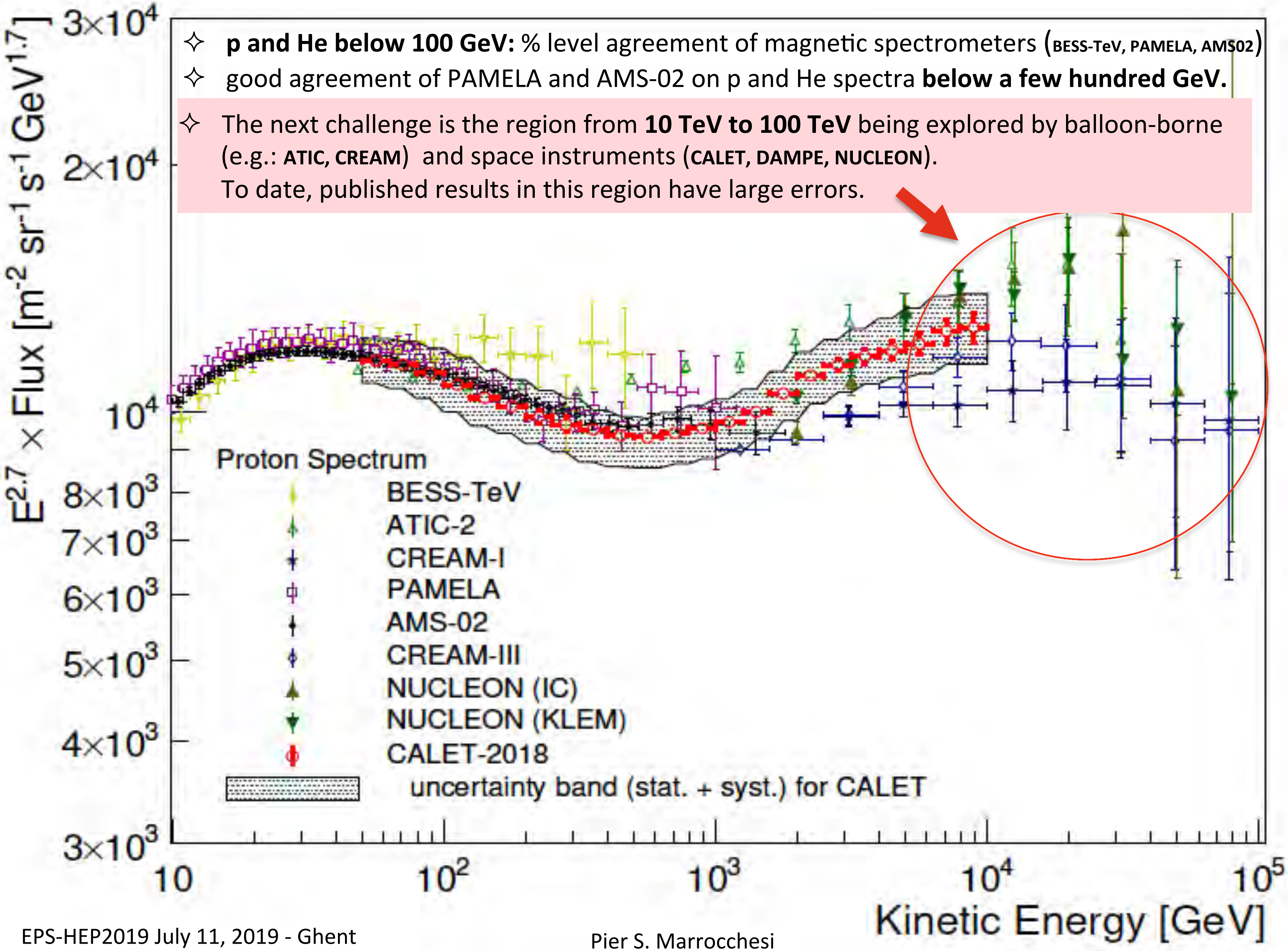

Charge Identification of Nuclei with CHD and IMC

Single element selection for p, He and light nuclei is achieved by CHD+IMC charge analysis.

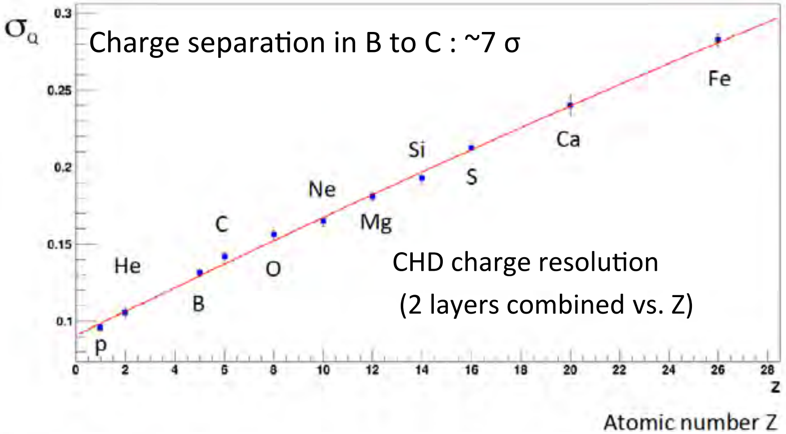

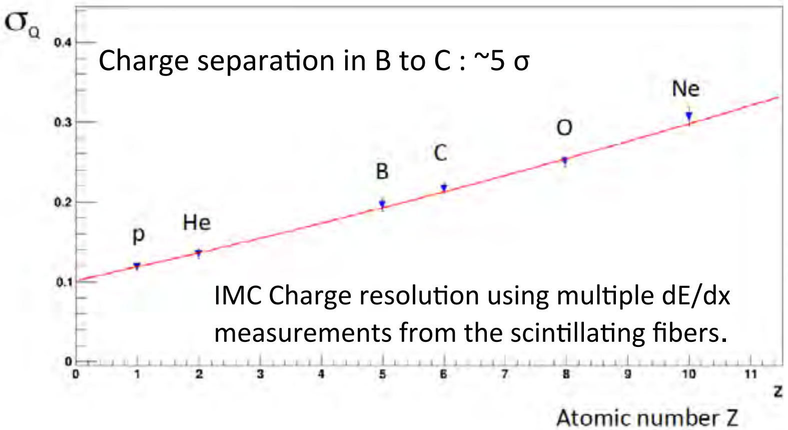

Deviation from Z^2 response is corrected both in CHD and IMC using a core + halo ionization model (Voltz)

Combined CHD-IMC proton-Helium charge-ID

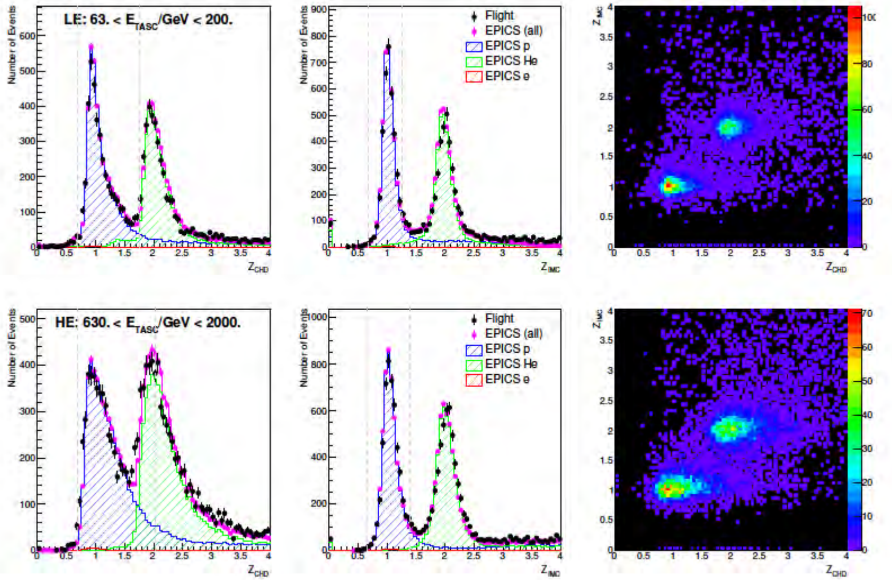

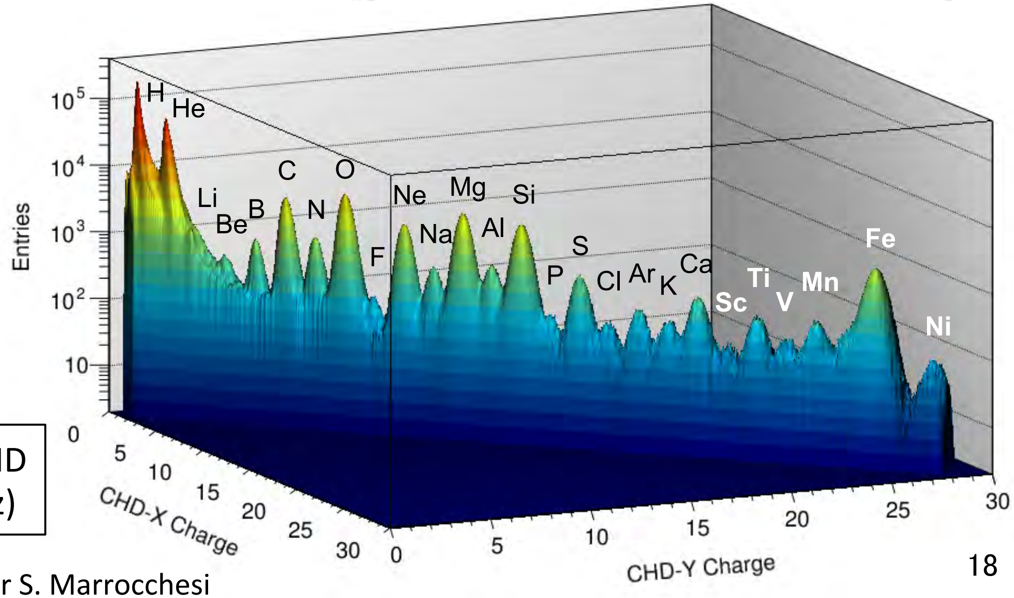

Preliminary fluxes of primary elements

Carbon and Oxygen

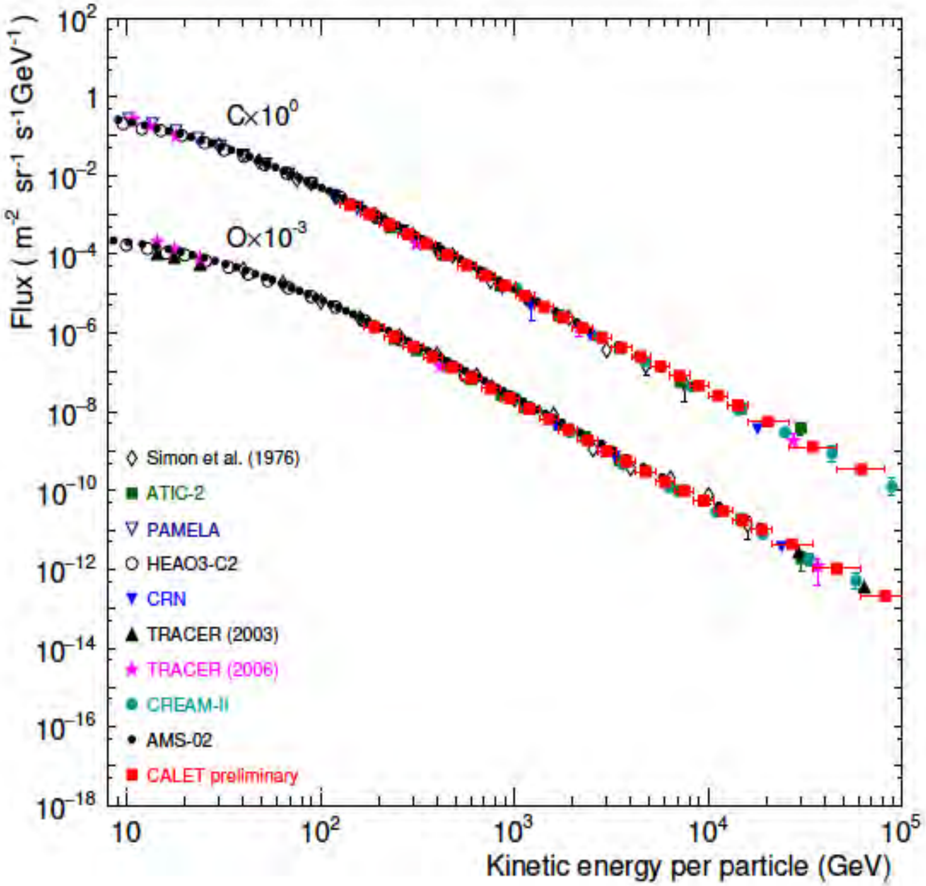

Ne, Mg, Si, S, Ca , Fe

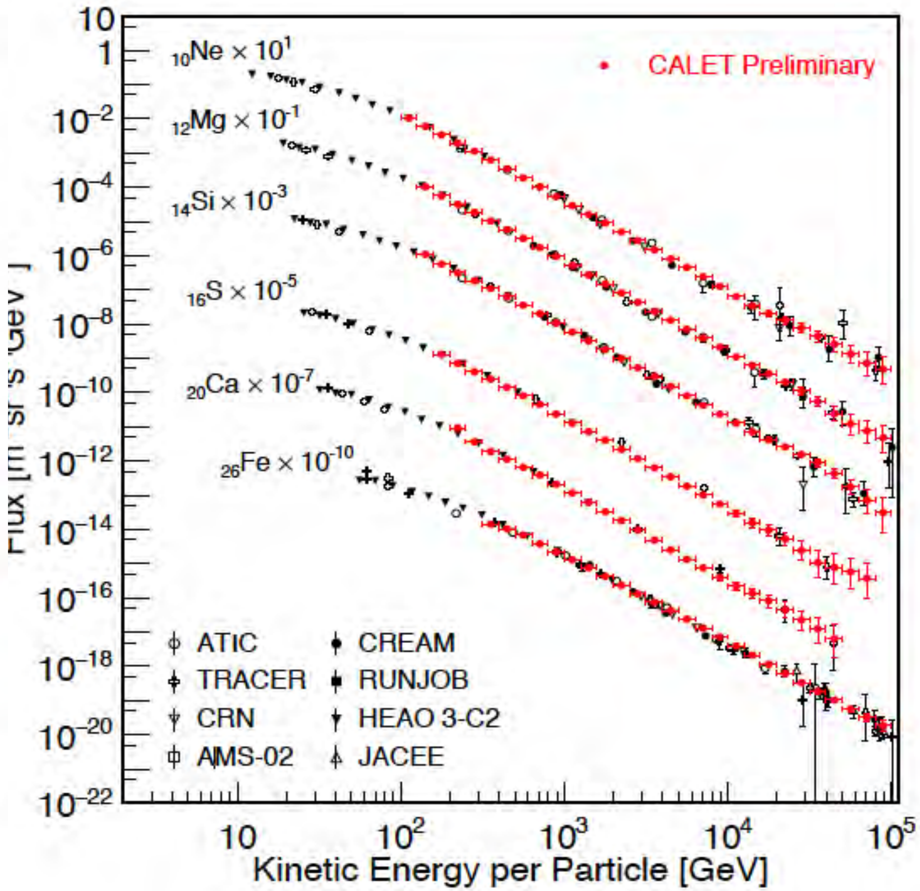

Preliminary Spectra of Z-even Nuclei from Ar to Ni (Z = 18-28)

[Y.Akaike, COSPAR 2018 E1.5-0028-18]

$_{18}$Ar

$_{20}$Ca

$_{22}$Ti

$_{24}$Cr

$_{26}$Fe

$_{28}$Ni

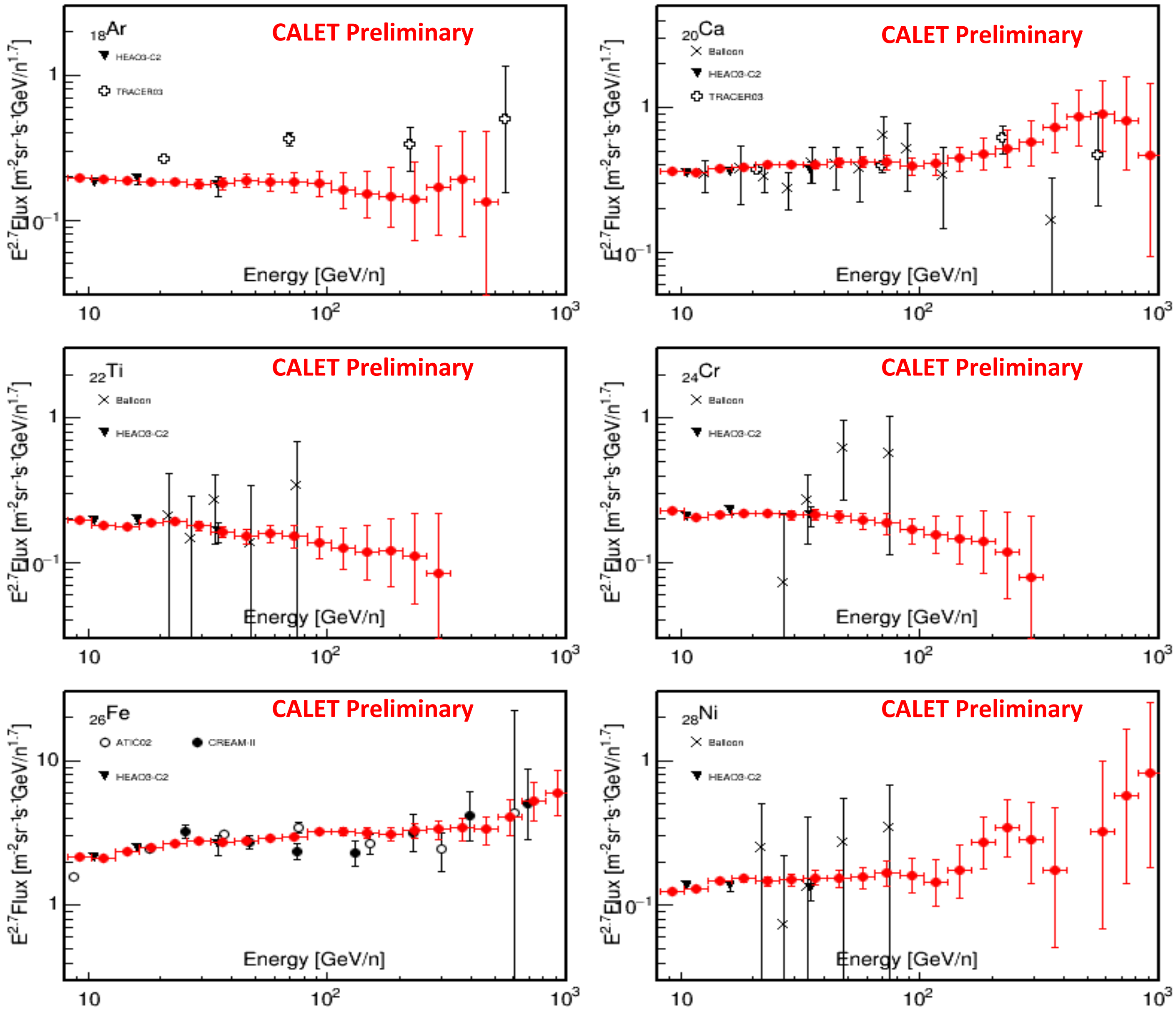

Preliminary Energy spectra of Carbon and Oxygen

(2 independent CALET analyses)

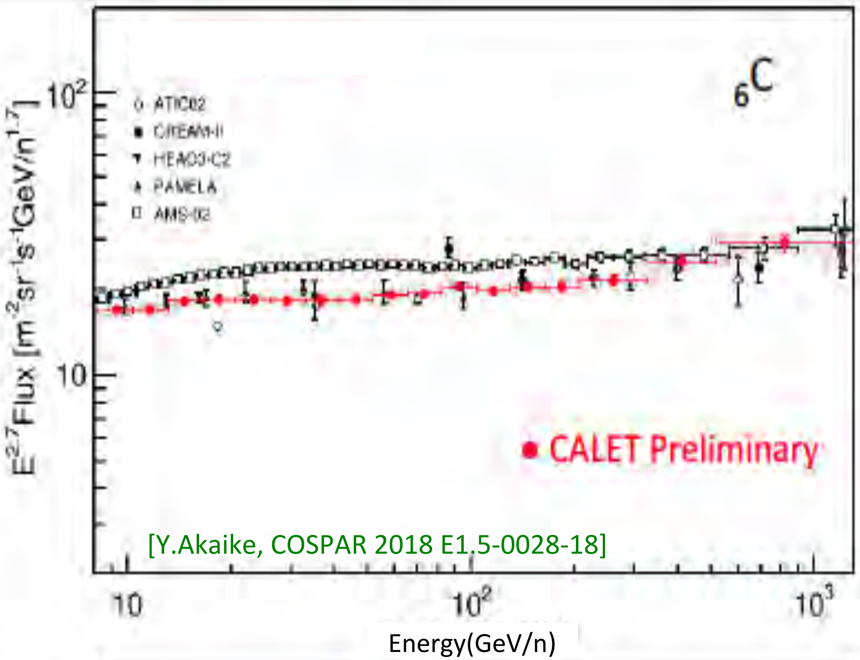

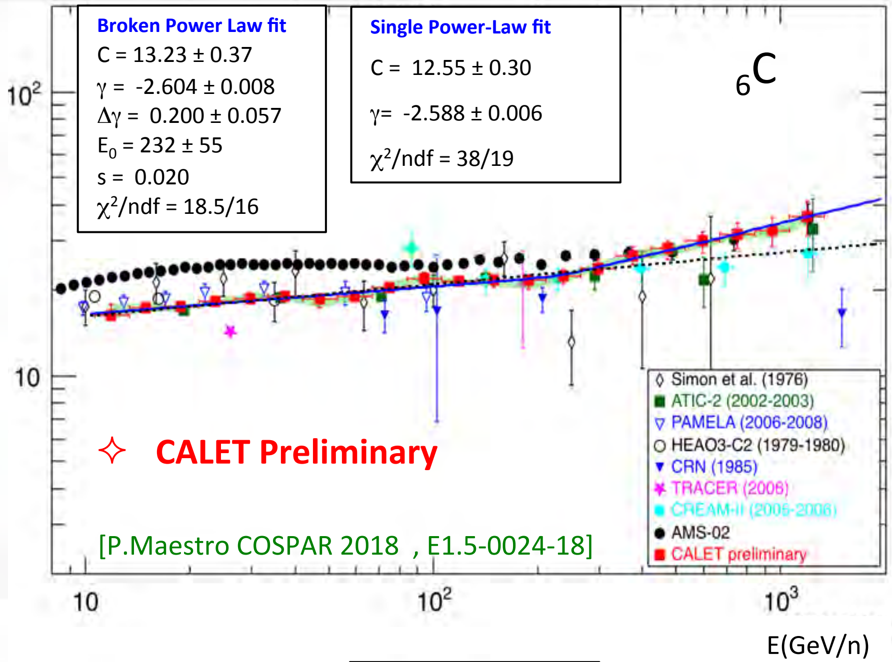

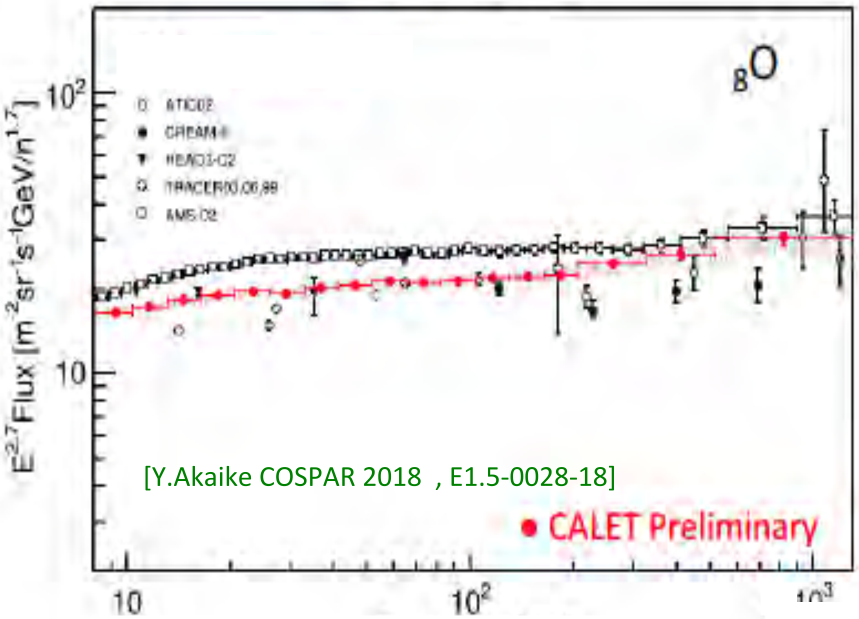

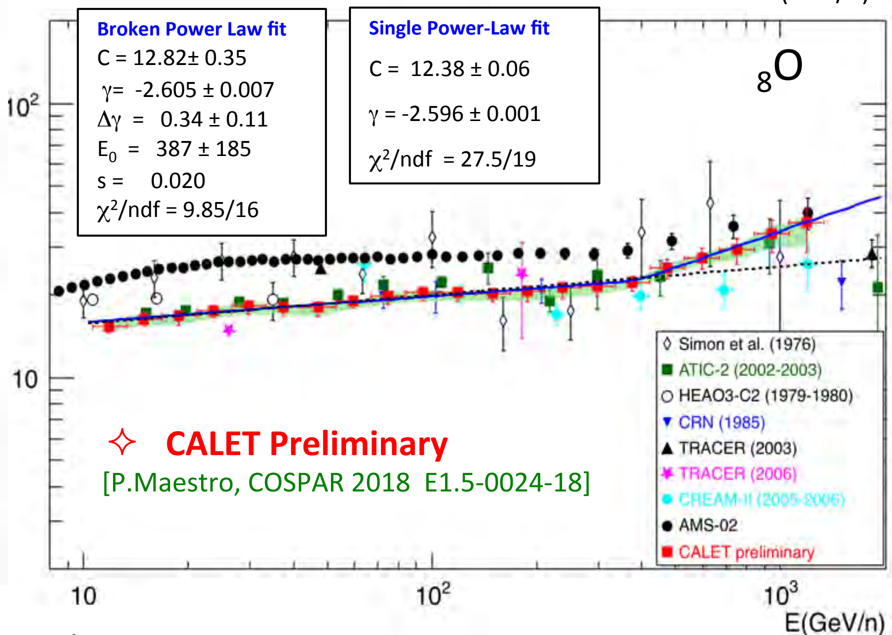

Boron-to-carbon flux ratio (Preliminary)

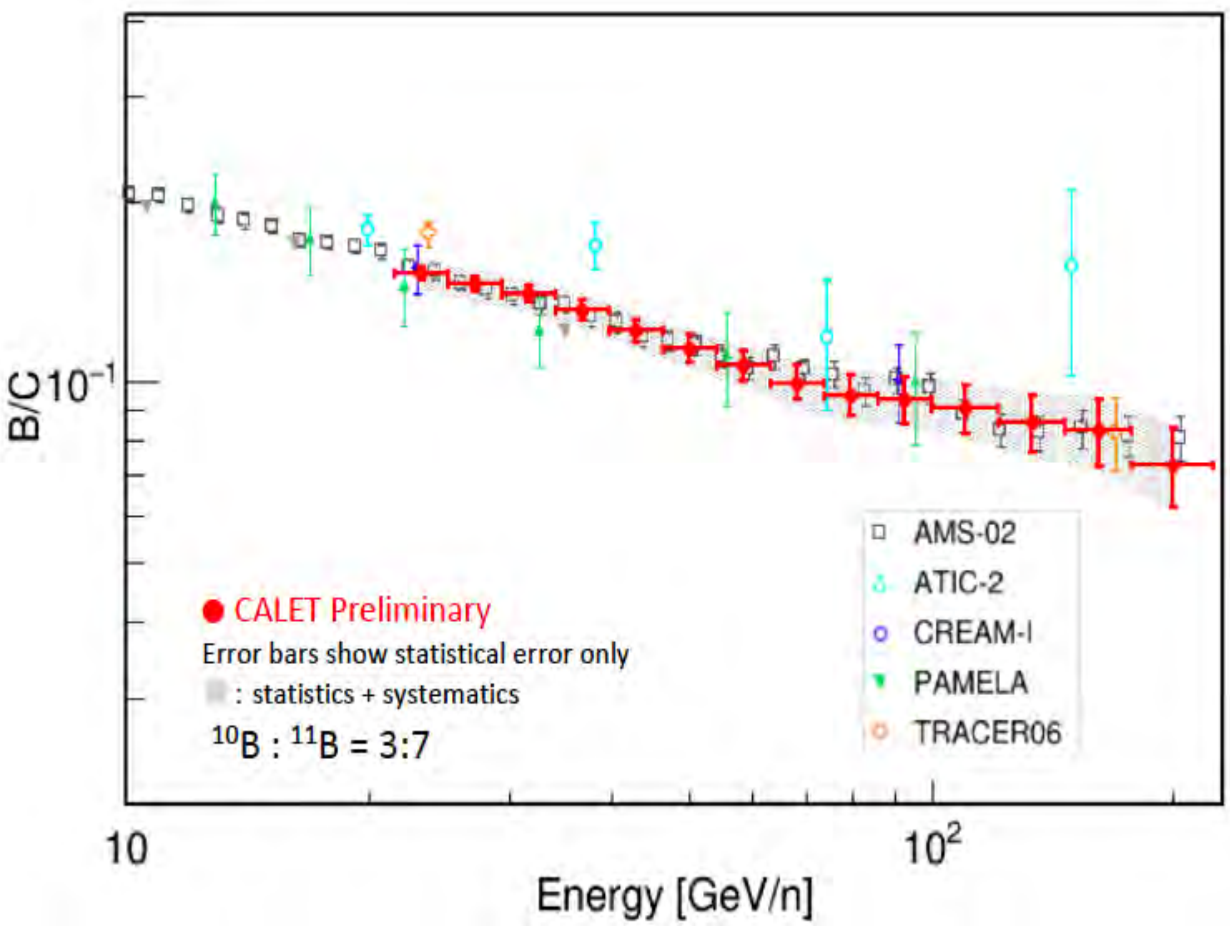

[Y. Akaike, APS April 14, 2019]

$^{10}B : ^{11}B = 3:7$

<u>Source of systematic uncertainties</u>

- Trigger efficiency
- Charge consistency cuts
- Track width selection
- Window range for charge identification
- Background model of p and He spectra
- Initial assuming spectra for energy unfolding
- Energy correction base on beam test results
- Difference of beam test model and flight model
- Long term stability

Ultra Heavy Nuclei (Preliminary Measurements for $26 < Z \leq 40$)

[B.Rauch, APS April 14, 2019]

CALET measures the relative abundances of nuclei above Fe through $_{40}$Zr

CALET has a special UH CR trigger utilizing the CHD and the top 4 layers of the IMC that:

- has an expanded geometry factor of ~4000 cm^{2}sr
- has a very high duty cycle due to low event rate

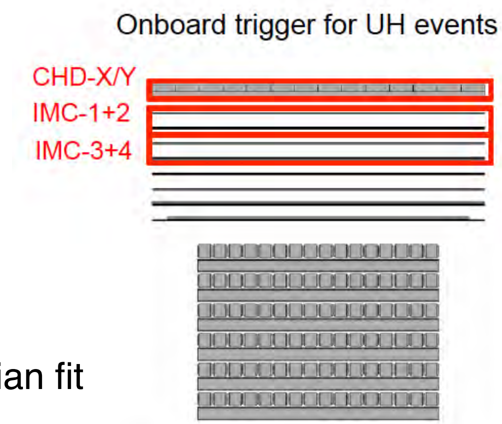

Data analysis

- ☐ Event Selection: Vertical cutoff rigidity > 4GV & Zenith Angle < 60 degrees
- ☐ Contamination from neighboring charge are determined by multiple-Gaussian fit

✧ The CALET UH element ratios relative to $_{26}$Fe show good agreement with SuperTIGER and ACE abundances.

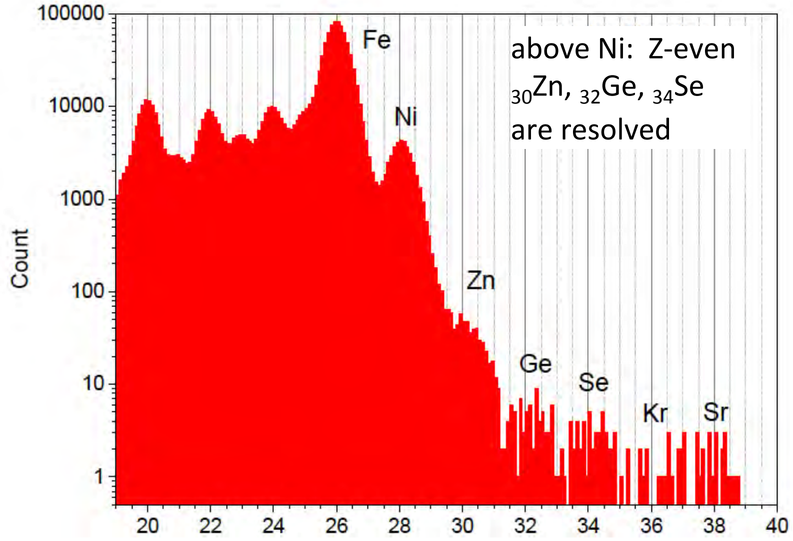

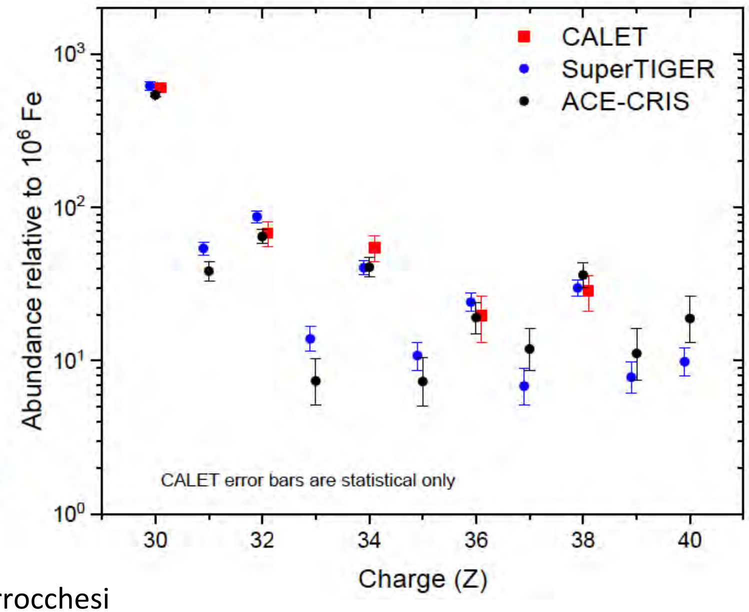

CALET γ–ray Sky (>1GeV)

Instrument characterized using EPICS simulations

- Effective area ~400 cm^2 above 2 GeV
- Angular resolution < 2° above 1 GeV (< 0.2° above 10 GeV)
- Energy resolution ~12% at 1 GeV (~5% at 10 GeV)

Simulated IRFs consistent with 2 years of flight data

Consistency in signal-dominated regions with Fermi-LAT

Residual background in low-signal regions

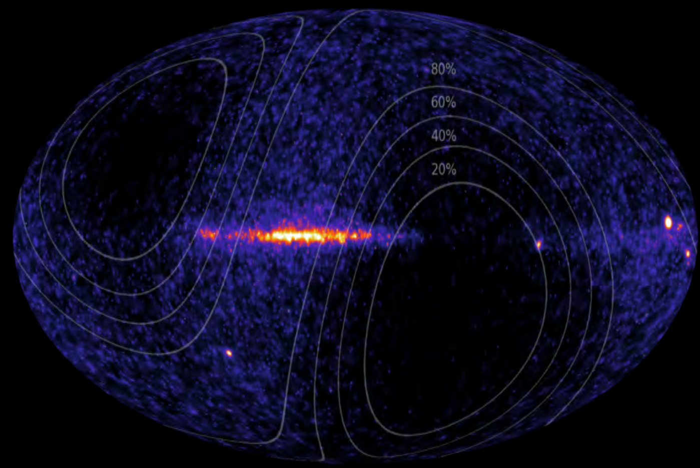

[N.Cannady, COSPAR 2018 E1.17-0009-18]

Flux validation with pulsars (under investigation)

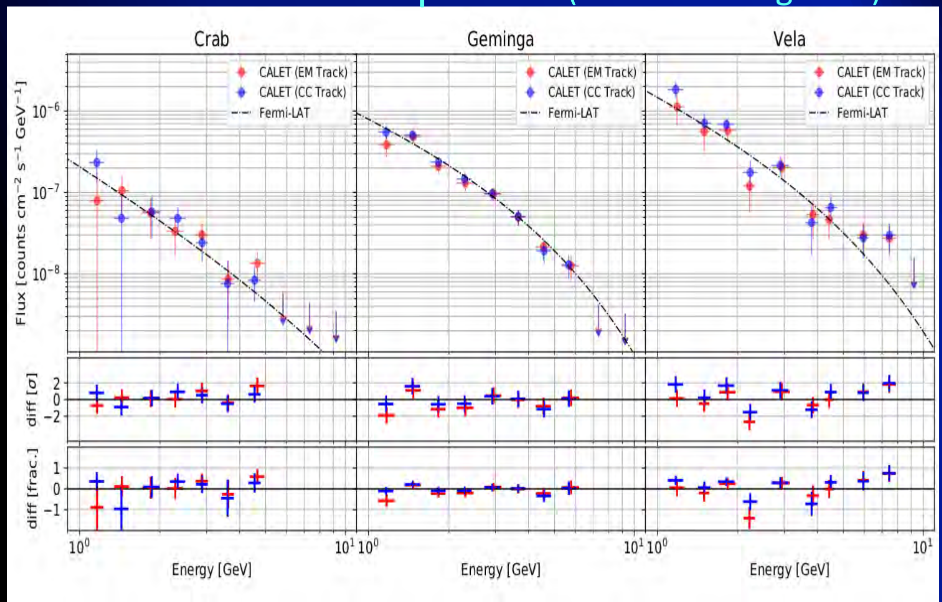

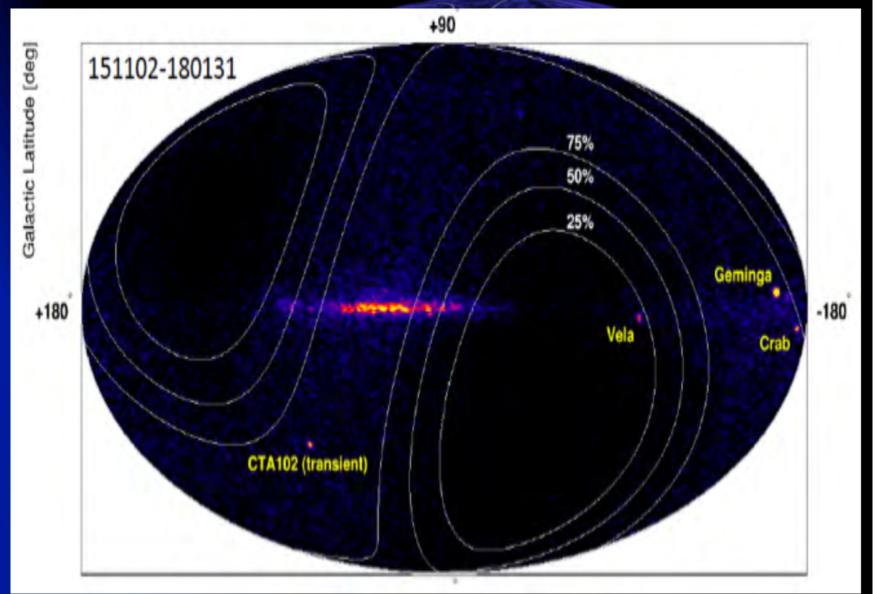

CALET Gamma-ray Burst Monitor (CGBM)

Hard X-ray Monitor (HXM)

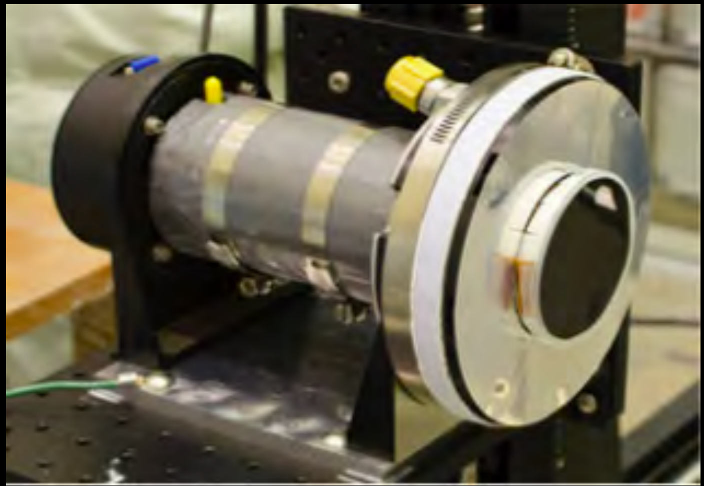

Soft Gamma-ray Monitor (SGM)

	HXM (x2)	SGM
Detector (Crystal)	$LaBr_3$(Ce)	BGO
Number of detectors	2	1
Diameter [mm]	61	102
Thickness [mm]	12.7	76
Energy range [keV]	7-1000	100-20000
Energy resolution@662 keV	~3%	~15%
Field of view	~3 sr	~2π sr

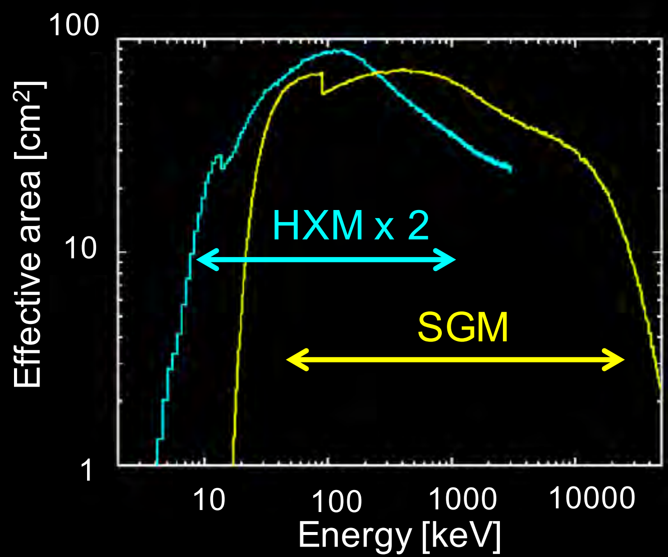

CGBM Observations Summary

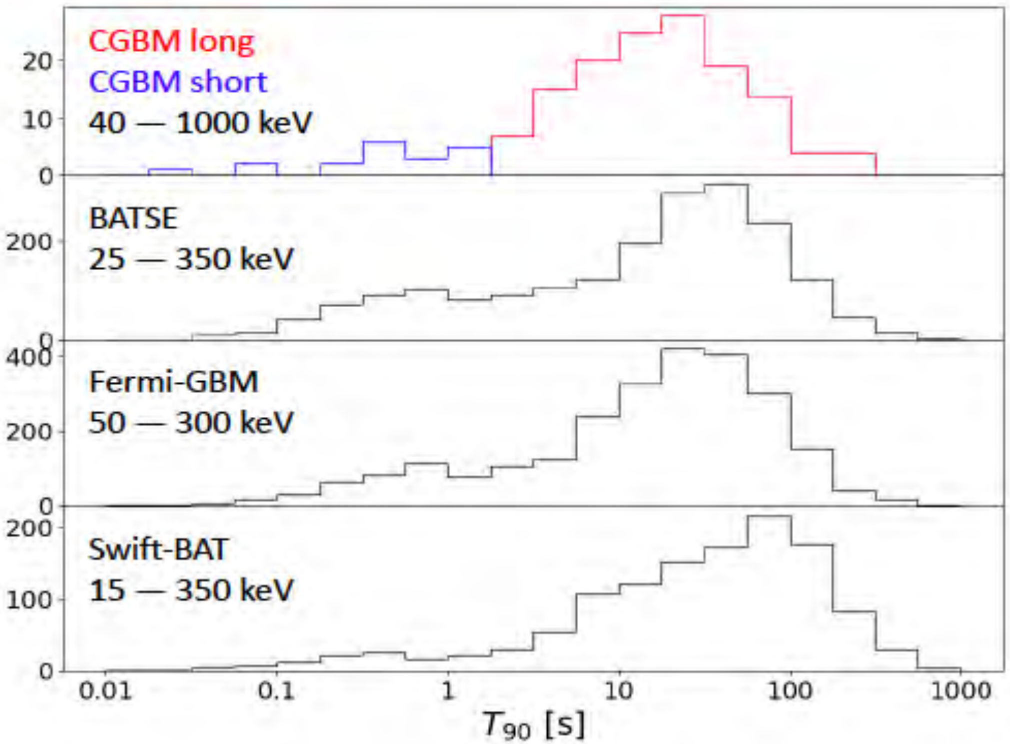

Examples of LIght Curves

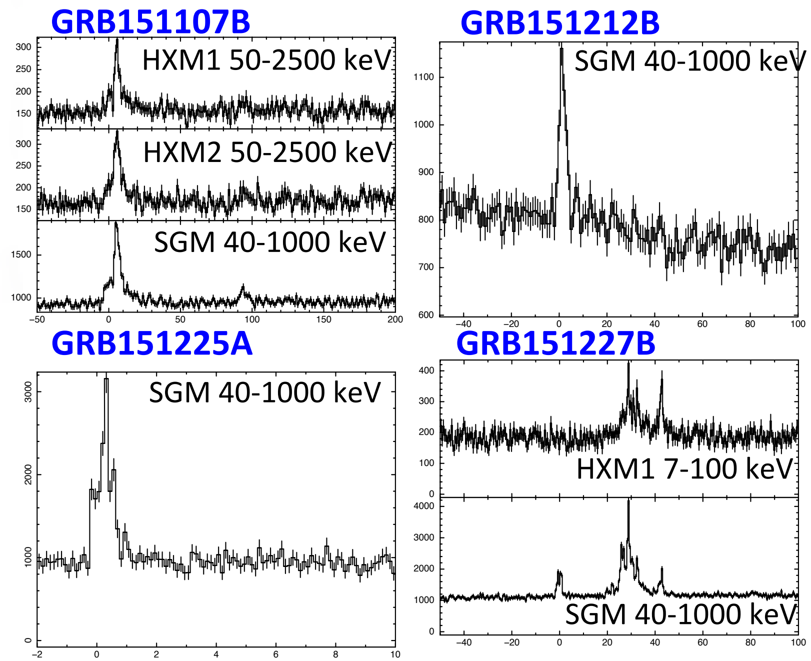

- ✧ As of June 2019:

  159 GRBs detected

  140 Long (88%) **19 Short (12%)**

  Average rate ~ **43 GRBs/year**

Raw count spectra of **GRB 160625B**

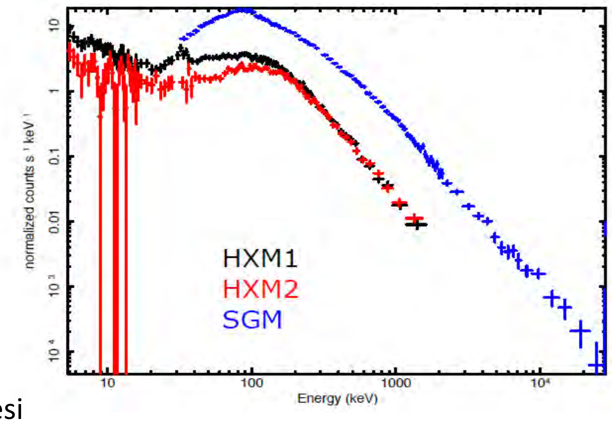

Complete Search Results for GW Events during O1&O2

GW151226: O. Adriani et al. (CALET Collaboration), ApJL 829:L20 (2016).
All O1 & O2: O. Adriani et al. (CALET Collaboration), ApJ 863 (2018) 160.

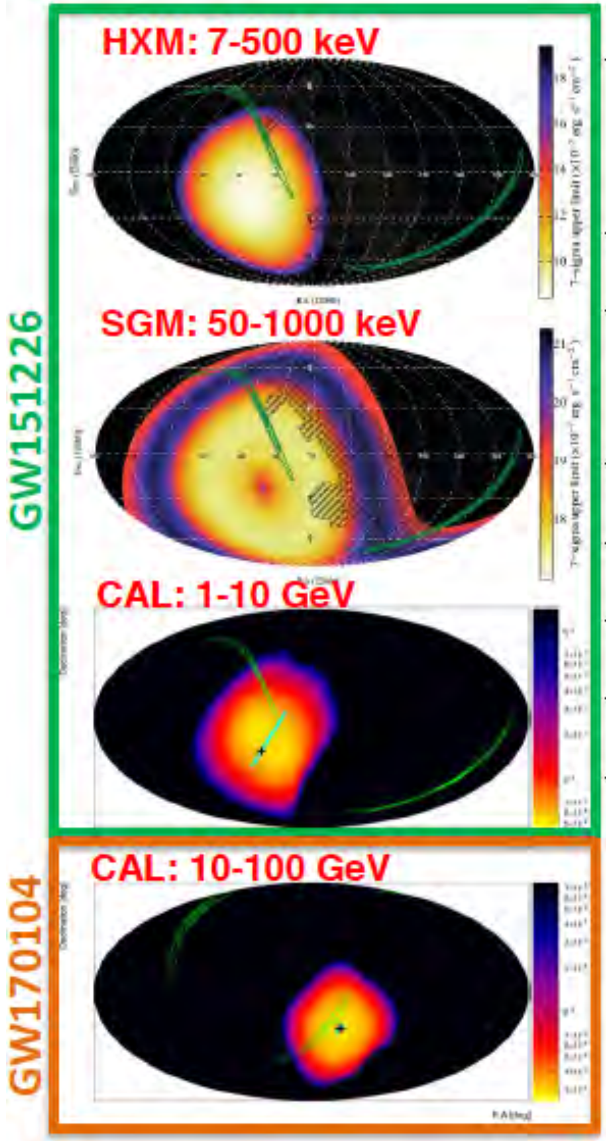

Event	Type	Mode	Sum. LIGO prob.	Obs. time	Upper limits	
					Ene. Flux erg cm^{-2} s^{-1}	Lum. erg s^{-1}
GW150914	BH-BH	Before operation				
GW151226	BH-BH	LE HXM SGM	15%	T_0-525 – T_0+211	9.3 x 10^{-8} 1.0 x 10^{-6} 1.8 x 10^{-6}	2.3 x 10^{48} 3-5 x 10^{49}
GW170104	BH-BH	HE	30%	T_0-60 – T_0+60	6.4 x 10^{-6}	6.2 x 10^{50}
GW170608	BH-BH	HE	0%	T_0-60 – T_0+60	Out of FOV	
GW170814	BH-BH	HE	0%	T_0-60 – T_0+60	Out of FOV	
GW170817	NS-NS	HE	0%	T_0-60 – T_0+60	Out of FOV	

- CALET can search for EM counterparts to LIGO/Virgo triggers
- All O1 and O2 triggers checked – no signal in CGBM or CAL
- Upper limits set for GW151226 for CGBM+CAL in 2016 paper
- Upper limits for the CAL set using refined LE selection for triggers to-date in the 2018 paper

CALET: Summary and Future Prospects

- CALET was successfully launched on Aug. 19th, 2015. The observation campaign started on Oct. 13th, 2015. Excellent performance and remarkable stability of the instrument.
- As of May 31, 2019 total observation time is 1327 days with live time fraction to total time close to 84%. Nearly 1.8 billion events collected with low (> 1 GeV) + high energy (>10 GeV) triggers.
- In-flight calibrations with p & He events + CERN beam tests with e, p and fragmented ions + linearity in the energy measurements established up to 10^6 MIP.
- Measurement of electron+positron spectrum in 11 GeV - 4.8 TeV range using full acceptance Observation of a flux reduction above 1 TeV.
- Direct measurement of proton spectrum in 50 GeV – 10 TeV energy range. Spectral hardening observed above a few hundred GeV.
- Preliminary analysis of primary elements up to Fe and secondary-to-primary ratios.
- Preliminary analysis of UH cosmic rays up to Z=40.
- Study of diffuse and point sources with gamma-rays. Follow-up observations of GW events in X-ray and gamma-ray bands. CALET's CGBM detected 159 GRBs in the energy range 7 keV-20 MeV.
- After an initial period of 2 years CALET observation time has been extended to 5 years at least.

Thank you
for your attention !

CALET Collaboration Team

O. Adriani[25], Y. Akaike[2], K. Asano[7], Y. Asaoka[9,31], M.G. Bagliesi[29], E. Berti[25], G. Bigongiari[29], W.R. Binns[32], S. Bonechi[29], M. Bongi[25], P. Brogi[29], A. Bruno[15], J.H. Buckley[32], N. Cannady[13], G. Castellini[25], C. Checchia[26],M.L. Cherry[13], G. Collazuol[26], V. Di Felice[28], K. Ebisawa[8], H. Fuke[8], T.G. Guzik[13], T. Hams[3], N. Hasebe[31], K. Hibino[10], M. Ichimura[4], K. Ioka[34], W. Ishizaki[7], M.H. Israel[32], K. Kasahara[31], J. Kataoka[31], R. Kataoka[17], Y. Katayose[33], C. Kato[23], Y.Kawakubo[1], N. Kawanaka[30], K. Kohri [12], H.S. Krawczynski[32], J.F. Krizmanic[2], T. Lomtadze[27], P. Maestro[29], P.S. Marrocchesi[29], A.M. Messineo[27], J.W. Mitchell[15], S. Miyake[5], A.A. Moiseev[3], K. Mori[9,31], M. Mori[21], N. Mori[25], H.M. Motz[31], K. Munakata[23], H. Murakami[31], S. Nakahira[20], J. Nishimura[8], G.A De Nolfo[15], S. Okuno[10], J.F. Ormes[25], S. Ozawa[31], L. Pacini[25], F. Palma[28], V. Pal'shin[1], P. Papini[25], A.V. Penacchioni[29], B.F. Rauch[32], S.B. Ricciarini[25], K. Sakai[3], T. Sakamoto[1], M. Sasaki[3], Y. Shimizu[10], A. Shiomi[18], R. Sparvoli[28], P. Spillantini[25], F. Stolzi[29], S. Sugita[1], J.E. Suh[29], A. Sulaj[29], I. Takahashi[11], M. Takayanagi[8], M. Takita[7], T. Tamura[10], N. Tateyama[10], T. Terasawa[7], H. Tomida[8], S. Torii[9,31], Y. Tunesada[19], Y. Uchihori[16], S. Ueno[8], E. Vannuccini[25], J.P. Wefel[13], K. Yamaoka[14], S. Yanagita[6], A. Yoshida[1], and K. Yoshida[22]

1) Aoyama Gakuin University, Japan
2) CRESST/NASA/GSFC and Universities Space Research Association, USA
3) CRESST/NASA/GSFC and University of Maryland, USA
4) Hirosaki University, Japan
5) Ibaraki National College of Technology, Japan
6) Ibaraki University, Japan
7) ICRR, University of Tokyo, Japan
8) ISAS/JAXA Japan
9) JAXA, Japan
10) Kanagawa University, Japan
11) Kavli IPMU, University of Tokyo, Japan
12) KEK, Japan
13) Louisiana State University, USA
14) Nagoya University, Japan
15) NASA/GSFC, USA
16) National Inst. of Radiological Sciences, Japan
17) National Institute of Polar Research, Japan
18) Nihon University, Japan
19) Osaka City University, Japan
20) RIKEN, Japan
21) Ritsumeikan University, Japan
22) Shibaura Institute of Technology, Japan
23) Shinshu University, Japan
24) University of Denver, USA
25) University of Florence, IFAC (CNR) and INFN, Italy
26) University of Padova and INFN, Italy
27) University of Pisa and INFN, Italy
28) University of Rome Tor Vergata and INFN, Italy
29) University of Siena and INFN, Italy
30) University of Tokyo, Japan
31) Waseda University, Japan
32) Washington University-St. Louis, USA
33) Yokohama National University, Japan
34) Yukawa Institute for Theoretical Physics, Kyoto University, Japan

CALET Collaboration Team

O. Adriani[25], Y. Akaike[2], K. Asano[7], Y. Asaoka[9,31], M.G. Bagliesi[29], E. Berti[25], G. Bigongiari[29],
W.R. Binns[32], S. Bonechi[29], M. Bongi[25], P. Brogi[29], A. Bruno[15], J.H. Buckley[32], N. Cannady[13],
G. Castellini[25], C. Checchia[26],M.L. Cherry[13], G. Collazuol[26], V. Di Felice[28], K. Ebisawa[8], H. Fuke[8], T.G. Guzik[13],
T. Hams[3], N. Hasebe[31], K. Hibino[10], M. Ichimura[4], K. Ioka[34], W. Ishizaki[7], M.H. Israel[32], K. Kasahara[31],
J. Kataoka[31], R. Kataoka[17], Y. Katayose[33], C. Kato[23], Y.Kawakubo[1], N. Kawanaka[30], K. Kohri [12], H.S. Krawczynski[32],
J.F. Krizmanic[2], T. Lomtadze[27], P. Maestro[29], P.S. Marrocchesi[29], A.M. Messineo[27], J.W. Mitchell[15], S. Miyake[5],
A.A. Moiseev[3], K. Mori[9,31], M. Mori[21], N. Mori[25], H.M. Motz[31], K. Munakata[23], H. Murakami[31], S. Nakahira[20],
J. Nishimura[8], G.A De Nolfo[15], S. Okuno[10], J.F. Ormes[25], S. Ozawa[31], L. Pacini[25], F. Palma[28], V. Pal'shin[1],
P. Papini[25], A.V. Penacchioni[29], B.F. Rauch[32], S.B. Ricciarini[25], K. Sakai[3], T. Sakamoto[1],
M. Sasaki[3], Y. Shimizu[10], A. Shiomi[18], R. Sparvoli[28], P. Spillantini[25], F. Stolzi[29], S. Sugita[1], J.E. Suh[29],
A. Sulaj[29], I. Takahashi[11], M. Takayanagi[8], M. Takita[7], T. Tamura[10], N. Tateyama[10], T. Terasawa[7],
H. Tomida[8], S. Torii[9,31], Y. Tunesada[19], Y. Uchihori[16], S. Ueno[8], E. Vannuccini[25], J.P. Wefel[13],
K. Yamaoka[14], S. Yanagita[6], A. Yoshida[1], and K. Yoshida[22]